



Deletion of *Maged1* in mice abolishes locomotor and reinforcing effects of cocaine

Jean-François De Backer^{1,†} , Stéphanie Monlezun^{1,‡}, Bérangère Detraux¹, Adeline Gazan¹, Laura Vanopdenbosch¹, Julian Cheron¹, Giuseppe Cannazza², Sébastien Valverde³, Lídia Cantacors⁴, Mérie Nassar⁵, Laurent Venance^{5,¶}, Olga Valverde^{4,¶}, Philippe Faure^{3,¶}, Michele Zoli^{6,¶}, Olivier De Backer^{7,¶}, David Gall^{1,§,¶}, Serge N Schiffmann^{1,¶} & Alban de Kerchove d'Exaerde^{1,8,*} 

Abstract

Melanoma antigen genes (*Mage*) were first described as tumour markers. However, some of *Mage* are also expressed in healthy cells where their functions remain poorly understood. Here, we describe an unexpected role for one of these genes, *Maged1*, in the control of behaviours related to drug addiction. Mice lacking *Maged1* are insensitive to the behavioural effects of cocaine as assessed by locomotor sensitization, conditioned place preference (CPP) and drug self-administration. Electrophysiological experiments in brain slices and conditional knockout mice demonstrate that *Maged1* is critical for cortico-accumbal neurotransmission. Further, expression of *Maged1* in the prefrontal cortex (PFC) and the amygdala, but not in dopaminergic or striatal and other GABAergic neurons, is necessary for cocaine-mediated behavioural sensitization, and its expression in the PFC is also required for cocaine-induced extracellular dopamine (DA) release in the nucleus accumbens (NAc). This work identifies *Maged1* as a critical molecule involved in cellular processes and behaviours related to addiction.

Keywords amygdala; dopamine; drug sensitization; nucleus accumbens; prefrontal cortex

Subject Category Neuroscience

DOI 10.15252/embr.201745089 | Received 30 August 2017 | Revised 20 June 2018 | Accepted 21 June 2018 | Published online 12 July 2018

EMBO Reports (2018) 19: e45089

See also: **M Loureiro & C Lüscher** (September 2018)

Introduction

The repeated use of drugs of abuse in predisposed individuals can lead to addiction, a psychiatric disorder in which patient loses control over substance consumption [1]. Addictive drugs increase extracellular DA levels in the mesocorticolimbic circuit [2] and share this ability despite varied pharmacological properties and mechanisms of action [3]. The extracellular DA increase caused by these drugs is thought to trigger an addictive state by inducing complex and long-lasting neural adaptations in the mesocorticolimbic circuit. Among adaptations that have been identified, drug intake causes changes in the synaptic strength of glutamatergic inputs onto DA neurons of the ventral tegmental area (VTA) and onto medium spiny neurons of the NAc [4]. In the NAc, early withdrawal (24 h) after repeated cocaine administration causes synaptic depression of glutamatergic transmission. After ~2 weeks of abstinence, these synapses switch from a depressed state to strengthened glutamate transmission [5]. They switch back to a depressed state after a subsequent cocaine challenge [6]. These forms of cocaine-induced plasticity at cortico-accumbal synapses have been shown to be causally related to addictive behaviours [7–9]. Mechanistically, multiple signalling pathways initiated by the activation of DA and glutamate receptors [10] drive the physiological changes induced by drugs of abuse. Manipulation of these pathways in transgenic mice has considerably improved our understanding of the molecular basis of addiction. For example, this approach has been used to confirm the primary molecular targets of drugs of abuse such as the DA transporter (DAT) for cocaine [11].

- Laboratoire de Neurophysiologie, ULB Neuroscience Institute, Université Libre de Bruxelles (ULB), Brussels, Belgium
 - Dipartimento di Scienze della Vita, Centro di Neuroscienze e Neurotecnologie, Università degli Studi di Modena e Reggio Emilia, Modena, Italy
 - INSERM, CNRS, Neuroscience Paris Seine - Institut de Biologie Paris Seine (NPS - IBPS), UPMC Univ Paris 06, Sorbonne Universités, Paris, France
 - Departament de Ciències Experimentals i de la Salut, Grup de Recerca en Neurobiologia del Comportament (GReNeC), Institut Hospital del Mar d'Investigacions Mèdiques (IMIM), Universitat Pompeu Fabra, Barcelona, Spain
 - Center for Interdisciplinary Research in Biology, Collège de France, INSERM U1050, CNRS UMR7241, Labex Memolife, Paris, France
 - Dipartimento di Scienze Biomediche, Metaboliche e Neuroscienze, Centro di Neuroscienze e Neurotecnologie, Università degli Studi di Modena e Reggio Emilia, Modena, Italy
 - URPHYM (Unité de Recherche en Physiologie Moléculaire), NARILIS (Namur Research Institute for Life Sciences), Université de Namur, Namur, Belgium
 - WELBIO, Brussels, Belgium
- *Corresponding author. Tel: +32 25554120; E-mail: adekerch@ulb.ac.be
 †These authors contributed equally to this work
 ‡Present address: Neuronal Circuits and Metabolism, Faculty of Animal Sciences, Technical University of Munich, Freising-Weihenstephan, Germany
 §Present address: Aelis Pharma, Bordeaux, France
 §Present address: Laboratory of Physiology and Pharmacology, ULB, Brussels, Belgium

The identification of new genes controlling the pathophysiological changes leading to addictive states represents an important method to unveil new molecular mechanisms underlying addiction-associated neuroadaptations. Here, we assessed the role of *Maged1* in electrophysiological and behavioural correlates of addiction. *Maged1* belongs to the large *Mage* family, first described as genes expressed in cancer and germ line cells [12]. Contrary to other *Mage* genes, *Maged1* is expressed in healthy somatic tissues, including the developing and adult central nervous system [13]. Recent studies have shown that *Maged1* is involved in the regulation of various and complex behavioural functions including regulation of circadian rhythms [14], social and sexual behaviours [15] and memory formation [16]. *Maged1* has also been implicated in neuropsychiatric conditions such as depression [17] and disorders of feeding behaviour [15]. In addition, the relevance of *Maged1* in cognitive functions has recently been enlightened in a human context. Indeed, mutations in *Maged1* were associated with intellectual disability in humans [18]. At the molecular level, a genome-wide analysis identified the promoter region of *Maged1* as a target of chromatin remodelling induced in the NAc by a chronic cocaine treatment [19]. In this study, the promoter of *Maged1* was found in the fourth position in a list of 213 promoters that co-precipitate with polyacetylated histones and with the activated form of cAMP response element binding protein (CREB), a transcription factor activated by cocaine and critical for behavioural responses to drugs of abuse [20]. Interestingly, *Maged1* binds directly to CREB in the hippocampus [16]. In addition, *Maged1* has been showed to interact with various partner proteins. At the plasma membrane, *Maged1* binds to the neurotrophin receptor p75 involved in neuronal developmental apoptosis [21]. It also modulates serotonin transporter ubiquitinylation, internalization and degradation by interacting with RING E3 ubiquitin ligase [17]. Given its roles in cognitive functions and its possible regulation by cocaine, we explored the involvement of *Maged1* in cocaine addiction by using mice lacking the functional *Maged1* allele (*Maged1*^{KO} [21]). We found that mice lacking *Maged1* were insensitive to cocaine in behavioural paradigms of addiction. These behavioural changes were accompanied by reduction of cocaine-induced DA overflow in the NAc. Depletion of *Maged1* selectively in PFC or amygdala, but not in DA or γ -aminobutyric acid (GABA) midbrain neurons or striatal neurons, partially reproduced this phenotype. This demonstrates that psychomotor effects of cocaine require the expression of *Maged1* in these brain regions.

Results

Altered sensitivity to cocaine in *Maged1*-deficient mice

We began our study by investigating the behavioural effects of cocaine in *Maged1*-deficient mice. As expected, the acute administration of cocaine (20 mg/kg of body weight, ip) induced a robust increase in locomotor activity in control mice. Repeated administrations of cocaine also elicited a progressive increase in locomotor activity, known as locomotor sensitization (Fig 1A). In contrast, the locomotor response to acute and chronic cocaine administration was completely abolished in *Maged1*^{KO} mice (Fig 1A).

As a previous study suggested that *Maged1*^{KO} mice demonstrate an altered response to reward in a sucrose preference test [17], we

assessed the rewarding effect of cocaine in these mice using the CPP paradigm. After conditioning, *Maged1*^{WT} mice developed a significant preference for the cocaine-paired compartment, whereas *Maged1*^{KO} animals did not (Fig 1B). While CPP is thought to be sensitive to drug reward, the most rigorous test of drug reinforcement with face-validity for human addiction is intravenous self-administration. We therefore tested *Maged1*^{KO} mice for their ability to self-administer cocaine. *Maged1*^{KO} mice learned to nose-poke normally to acquire food pellets (Fig 1C); however, only wild-type mice developed and maintained a reliable cocaine self-administration, whereas *Maged1*^{KO} mice did not acquire self-administration behaviour in response to cocaine (Fig 1D).

The observation that mice lacking *Maged1* were not sensitive to psychomotor or reinforcing effects of cocaine suggests these animals may have impairments in the function of the mesolimbic DA system, a brain circuit critical for the regulation of behaviours relevant to addiction [22]. As those dopaminergic circuits are also involved in the control of locomotion, we assessed motor functions in *Maged1*^{KO} mice. First, as expected from previous studies [15,17], the total distance travelled by *Maged1*^{KO} mice during the exploration of an open-field arena was decreased as compared to *Maged1*^{WT} mice (Fig 1E). Second, we assessed motor coordination using the accelerated rotarod test. In contrast to previous studies demonstrating normal motor behaviour in conditions of constant rotating speed [17], *Maged1*^{KO} mice were impaired in their ability to stay on an accelerating rotating rod, suggesting a deficit in motor coordination (Fig 1F). Despite this impairment, *Maged1*^{KO} mice were capable of learning motor skills and showed improvement in accelerating rotarod performance over days of training ($P < 0.0001$, Friedman test). These results show that mice lacking *Maged1* display motor defects in addition to an absence of behavioural responses to cocaine.

Alterations of dopamine transmission in *Maged1*-deficient mice

The common initial effect of drugs of abuse is to increase the extracellular concentration of DA in target nuclei of the mesocorticolimbic circuit, such as the NAc [2]. Given their absence of behavioural response to cocaine, we investigated DA levels in *Maged1*^{KO} mice by *in vivo* microdialysis. We found no difference in basal DA concentration in perfusates from the NAc of *Maged1*^{KO} mice as compared to their wild-type littermates (Fig 2A). We then assessed the increase in DA levels induced by a single cocaine injection (10 mg/kg, ip). This effect of cocaine was significantly reduced in *Maged1*^{KO} mice (Fig 2B). The impairment in the pharmacological response to cocaine could be due to alterations in DA synthesis, re-uptake or release or in the firing of dopaminergic neurons.

Striatal DA release results from the electrophysiological activity of neurons located in the midbrain. *In vivo*, these neurons fire with tonic or burst firing patterns [23,24]. Single-unit recordings in anaesthetized animals showed no significant effect of *Maged1* deletion on firing frequency of VTA DA neurons (Fig 2C). Moreover, there was no difference in burst firing, as assessed as the percentage of spikes within a burst (Fig 2C). We next tested whether the electrophysiological response of DA neurons to cocaine is preserved in *Maged1*^{KO} mice. At the somatic level (where electrophysiological recordings are performed), blocking the recapture of somatodendritically released DA results in the activation of somatodendritic D2

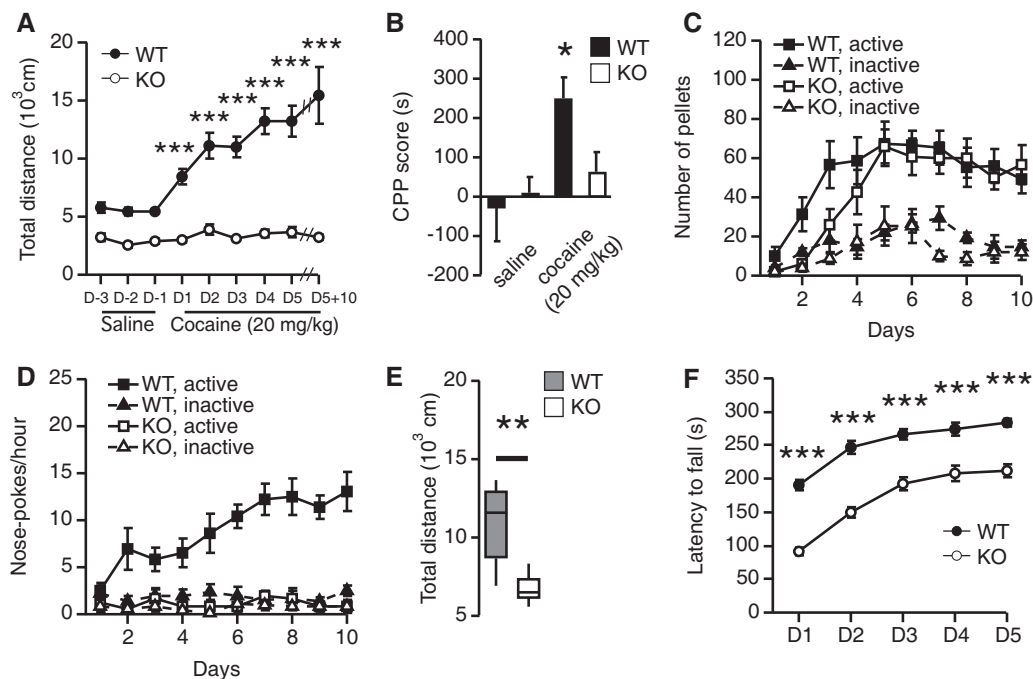


Figure 1. Behavioural characterization of *Maged1*^{KO} mice.

- A Locomotor sensitization to repeated cocaine injections (20 mg/kg, ip, mean \pm s.e.m., $n_{WT} = 7$, $n_{KO} = 8$; *Maged1*^{WT} versus *Maged1*^{KO}, $P < 0.0001$; time, $P < 0.0001$; interaction factor, $P < 0.0001$ repeated-measures two-way ANOVA; *** $P < 0.001$ as compared to *Maged1*^{WT}, Sidak's post-test).
- B Conditioned place preference for cocaine (20 mg/kg, ip) scored as the difference in time spent in the drug-paired compartment between post- and preconditioning tests (mean \pm s.e.m., $n_{WT, Sal.} = 4$, $n_{WT, Coc.} = 4$, $n_{KO, Sal.} = 4$, $n_{KO, Coc.} = 8$, *Maged1*^{WT} versus *Maged1*^{KO}, $P = 0.24$; treatment, $P = 0.0161$; interaction factor, $P = 0.08$, two-way ANOVA; * $P < 0.05$ as compared to saline, Tukey's post-test).
- C Acquisition of food-induced operant behaviour (mean \pm s.e.m., $n_{WT} = 6$, $n_{KO} = 6$; groups, $P = 0.0001$; time, $P < 0.0001$; interaction factor, $P < 0.0001$ repeated-measures two-way ANOVA; active versus inactive holes *Maged1*^{WT} $P = 0.0015$ and *Maged1*^{KO} $P = 0.0046$; active hole, *Maged1*^{WT} versus *Maged1*^{KO} $P = 0.68$, Tukey's post-test).
- D Cocaine self-administration (1 mg/kg/infusion, mean \pm s.e.m.; $n_{WT} = 9$, $n_{KO} = 10$, groups, $P < 0.0001$; time, $P < 0.0001$; interaction factor, $P < 0.0001$, repeated-measures two-way ANOVA; *Maged1*^{WT} active hole versus *Maged1*^{WT} inactive hole and *Maged1*^{KO} active and inactive holes $P < 0.001$, Tukey's post-test).
- E Total distance travelled during one hour spent in an open-field arena (boxplots represent median, first and third quartiles, whiskers indicating the maximal and minimal values observed, $n_{WT} = 8$, $n_{KO} = 8$, ** $P = 0.0011$, Mann-Whitney U test).
- F Motor coordination and motor skill learning on an accelerating rotarod (mean \pm SEM; $n_{WT} = 24$, $n_{KO} = 24$, *Maged1*^{WT} versus *Maged1*^{KO}, $P = 0.0001$; time, $P < 0.0001$; interaction factor, $P = 0.0196$, repeated-measures two-way ANOVA; *** $P < 0.001$ as compared to *Maged1*^{WT}, Sidak's post-test).

autoreceptors and thus in the inhibition of DA neurons in most VTA DA cells [25–27]. Indeed, an acute injection of cocaine (1 mg/kg, intravenous) induced a reduction of the DA neurons firing rate. This response was similar in *Maged1*^{WT} and *Maged1*^{KO} animals (Fig 2D). Taken together, these electrophysiological results indicate that deletion of *Maged1* did not disturb the firing properties of DA neurons of the VTA *in vivo*.

To determine the dynamics of vesicular release of DA, we next used fast-scan cyclic voltammetry to evaluate phasic DA release in acute striatal slices. The signal evoked by a single electrical stimulation of DA terminals was significantly increased in slices prepared from *Maged1*^{KO} mice compared to their wild-type control, suggesting an enhancement of vesicular DA release (Fig 2E and F). However, paired-pulse depression was preserved in slices from *Maged1*^{KO} mice while the response of trains of stimuli was enhanced (Fig EV1D and E).

We did not detect any difference in protein expression of the DAT, the primary molecular target of cocaine, between *Maged1*^{KO} and *Maged1*^{WT} mice (Fig EV2). As expected, the time constant of the exponential decay of the DA transient was not altered

in *Maged1*^{KO} mice, confirming normal DA uptake (Fig 2G). To determine if the behavioural insensitivity to cocaine observed in *Maged1*^{KO} mice was also present at the neurochemical level, we measured evoked DA transients following bath application of cocaine. Slices prepared from *Maged1*^{KO} mice reacted normally to cocaine showing that the lack of *Maged1* did not affect the effectiveness of cocaine at blocking the DAT (Fig EV1A–C).

Overall, *Maged1*^{KO} mice showed a dramatic impairment in cocaine-elicited increase in DA extracellular levels in the NAc, though electrophysiological, neurochemical and functional features of DA mesolimbic transmission appeared substantially maintained.

Alterations of glutamate transmission in *Maged1*-deficient mice

Glutamate transmission is a second major player in the development of the addictive state that powerfully interacts with DA transmission [28]. Alterations in glutamate transmission, in particular in glutamatergic synapses in the NAc [29], may contribute to the observed insensitivity of *Maged1*^{KO} mice to cocaine reinforcing effects. Thus, we studied the involvement of *Maged1* in the physiology of glutamate

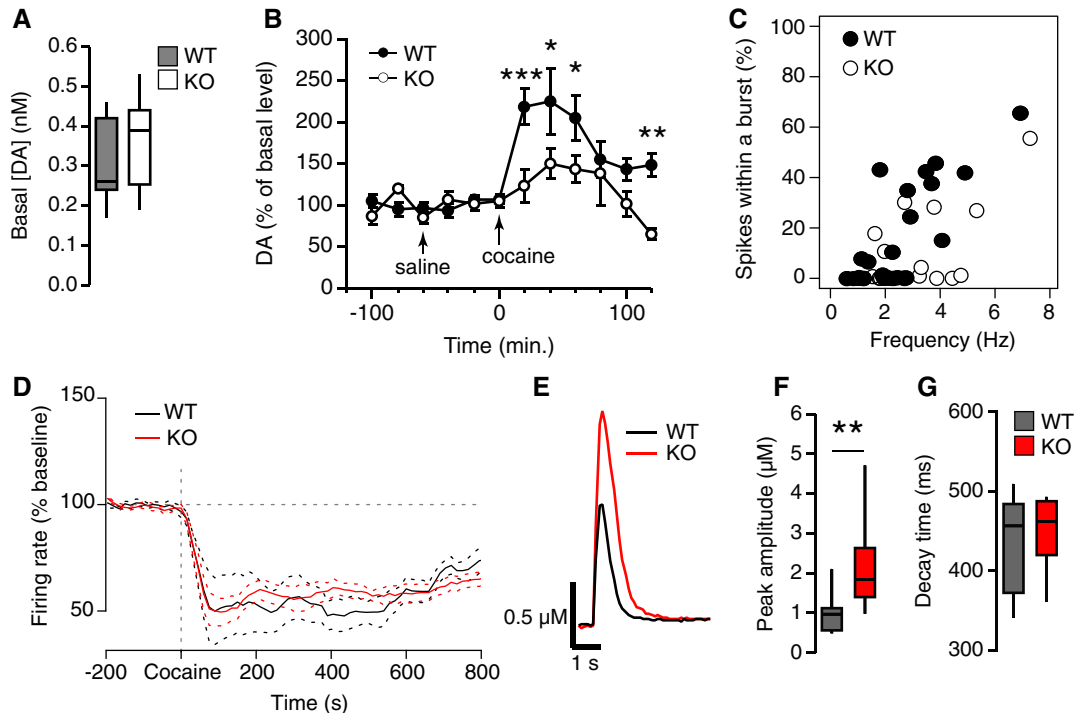


Figure 2. Characterization of DA transmission in *Maged1*^{KO} mice.

A, B Basal- (A) and cocaine-induced (10 mg/kg, ip) (B) increase in extracellular DA concentration in the NAc measured by *in vivo* microdialysis ($n_{WT} = 7$, $n_{KO} = 8$, Basal DA: $P = 0.71$, Mann–Whitney U test; Cocaine-evoked: mean \pm s.e.m., *Maged1*^{WT} versus *Maged1*^{KO}, $P = 0.003$; time, $P = 0.00036$; interaction factor, $P = 0.39$, repeated-measures two-way ANOVA; * $P < 0.05$, ** $P < 0.01$ *** $P < 0.001$ as compared to *Maged1*^{WT}, Sidak's post-test).

C Firing frequency-bursting plot of DA neurons recorded in the VTA in anaesthetized animals. The mean firing frequency is expressed against the percentage of spikes within a burst ($n_{WT} = 23$ cells from 10 mice, $n_{KO} = 26$ cells from 12 mice, $P_{\text{Frequency}} = 0.74$, $P_{\text{SWB}} = 0.061$, Mann–Whitney U test).

D Averaged \pm s.e.m. responses of VTA DA neurons to an acute cocaine injection (1 mg/kg, intravenous) recorded *in vivo* in anaesthetized *Maged1*^{WT} ($n = 20$ cells from 10 mice) and *Maged1*^{KO} animals ($n = 9$ cells from 8 animals).

E DA transients recorded in acute striatal slices by fast-scan cyclic voltammetry following a single electrical stimulus (averages of 8 traces each).

F, G Peak amplitude (F) and single exponential fit time constant of the decay phase (G) of DA transients ($n_{WT} = 12$ slices from 7 mice, $n_{KO} = 8$ slices from 4 mice, ** $P_{\text{Peak}} = 0.0054$, $P_{\text{Decay}} = 0.67$, Mann–Whitney U test).

Data information: Boxplots represent median, first and third quartiles, whiskers indicating the maximal and minimal values observed.

transmission in the NAc. We first recorded miniature excitatory currents (mEPSCs) in projection neurons that comprise ~95% of the neurons of the NAc. We found no difference in mEPSC amplitude or frequency between *Maged1*^{KO} and *Maged1*^{WT} mice (Fig 3A and B). However, the rise time and time constant of mEPSC decay were significantly increased in slices prepared from *Maged1*^{KO} mice, resulting in a significant increase in the amount of charge transferred through AMPA receptors (AMPA-R) during a quantal release event (Fig 3C and D). These changes could result from alterations in AMPA-R subunit composition or glutamate uptake, both of which could modify EPSCs kinetics without alterations in amplitude [30,31].

mEPSCs in NAc result from spontaneous glutamate release from axon terminals originating from multiple brain regions, including the PFC, hippocampus and amygdala. Each of these inputs has different properties and is differentially affected by cocaine [9] but effects of a specific connection, such as the cortico-accumbal synapses, can be masked in a NAc slice [6]. Thus, we next evoked EPSCs in the NAc by electrical stimulation of the fibres coming from the PFC in tilted parasagittal slices containing these two interconnected areas. In slices prepared from *Maged1*^{KO} mice, evoked EPSCs were slightly but not significantly smaller in control slices

(Fig EV3A and B). As evoked EPSCs are subject to variability as a function of the placement of the stimulating electrode and/or as a function of the fibre density, we computed the ratio between AMPA- and NMDA-mediated currents (A/N ratio) since this ratio provides a sensitive assay to detect differences in glutamatergic synaptic strength between experimental groups [6]. *Maged1*^{KO} mice displayed a significant decrease in the A/N ratio (Fig 3E and F), whereas the current–voltage relationship (I–V) was not altered (Fig 3E and G), suggesting changes in strength of PFC–NAc synaptic connections. We next tested the capacity of cortico-accumbal synapse to support synaptic plasticity. Consistent with previous reports (30), we observed that low-frequency stimulation (LFS, 1 Hz for 10 min) of layer 5 cortical cells induced long-term depression (LTD) in NAc output neurons from control mice, whereas an absence of synaptic plasticity was found in NAc output neurons from *Maged1*^{KO} mice (see examples in Fig 3H and summary curves in Fig 3I). However, somatic current injections in recorded pyramidal neurons of the PFC did not reveal any difference in their intrinsic excitability (Fig EV3C and D). Taken together, these results show that *Maged1*-deficient mice have severe abnormalities of glutamate transmission at cortico-accumbal synapses.

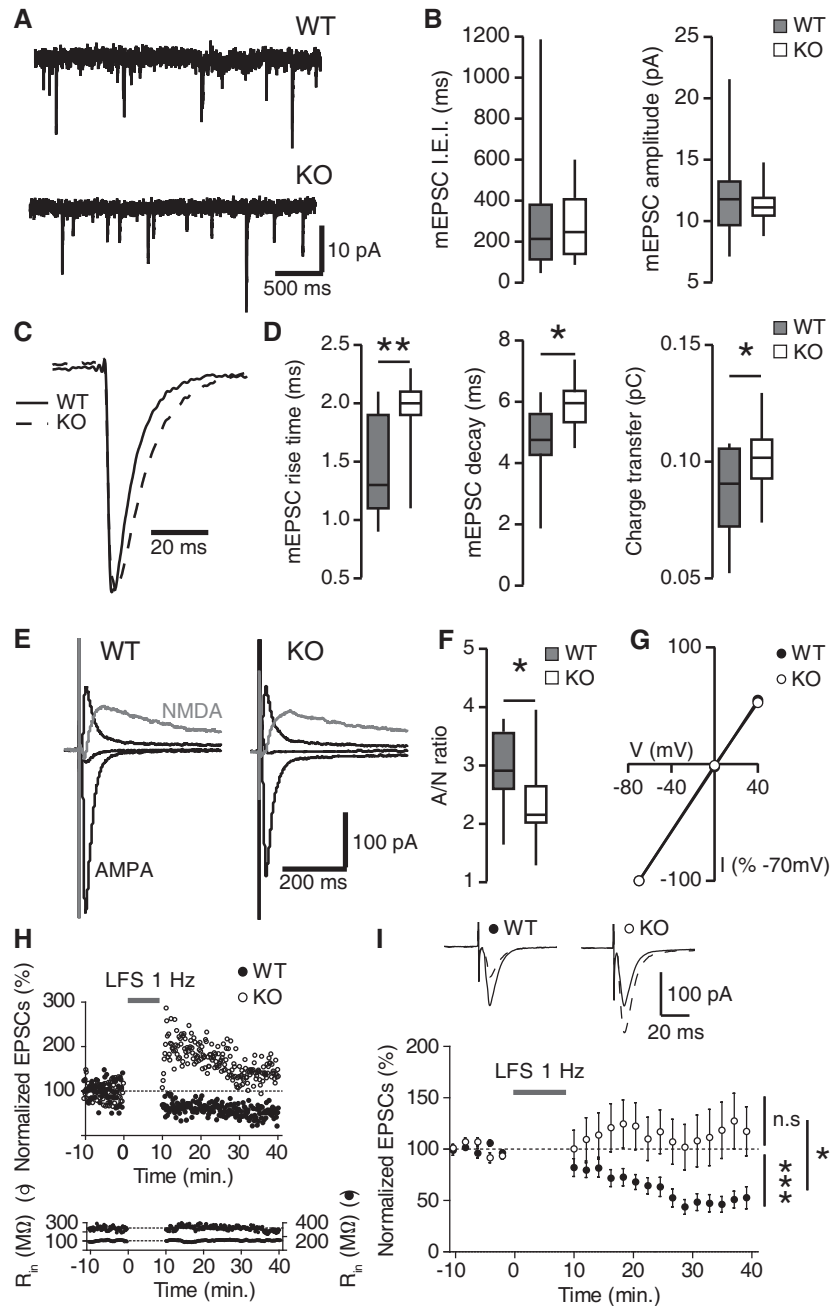


Figure 3. Electrophysiological characterization of glutamatergic transmission in projection neurons of the NAc in *Maged1*^{KO} mice.

- A Samples of mEPSCs recorded in acute brain slices prepared from *Maged1*^{WT} and *Maged1*^{KO} mice.
- B Distributions of mEPSCs inter-event intervals (I.E.I.) and amplitudes ($n_{WT} = 17$ cells from 6 mice, $n_{KO} = 15$ cells from 5 mice).
- C Superimposed, peak scaled mEPSCs averaged from 286 and 500 post-synaptic events recorded in neurons from *Maged1*^{WT} and *Maged1*^{KO} mice, respectively.
- D The rise time, the time constant of a single exponential fit of the decay phase and the amount of charges transferred were measured on averaged mEPSCs ($n_{WT} = 19$ cells from 6 mice, $n_{KO} = 15$ cells from 5 mice).
- E AMPA-R EPSCs evoked at -70 , 0 and $+40$ mV (black) and NMDA-R EPSCs (grey) recorded at $+40$ mV (averages from 10 traces each).
- F AMPA-R/NMDA-R currents peak ratios computed for the two groups.
- G Current–voltage relationships for AMPA-R EPSCs (mean \pm s.e.m., $n_{WT} = 10$ cells from nine mice, $n_{KO} = 14$ cells from 12 mice).
- H, I LTD was induced at cortico-accumbal synapses by LFS (1 Hz for 10 min) in control mice, whereas an absence of plasticity was observed in *Maged1*^{KO} mice. (H) Representative experiments. Upper panel, time courses of normalized EPSCs. Bottom panel, time courses of R_{in} . (I) Upper panel, representative traces are the average of 60 EPSCs during baseline (black traces) and between 20 and 30 min after LFS (dashed traces) from *Maged1*^{WT} and *Maged1*^{KO} mice (same cells as in H.). Lower panel, summary of LFS experiments (mean \pm s.e.m., $n = 9$ neurons from 6 *Maged1*^{WT} mice, and $n = 10$ neurons from 6 *Maged1*^{KO} mice). Significant different synaptic efficacy changes were observed between neurons from *Maged1*^{WT} and *Maged1*^{KO} subjected to LFS.

Data information: Boxplots represent median, first and third quartiles, whiskers indicating the maximal and minimal values observed. * $P < 0.05$, ** $P < 0.01$, *** $P < 0.0005$ (Mann–Whitney U test).

Selective deletion of *Maged1* in subsets of neurons

Present results show that conventional *Maged1*^{KO} mice have markedly reduced cocaine-elicited DA release from DA terminals of the NAC and abnormal glutamatergic transmission at cortico-accumbal synapses, suggesting that a profound dysfunction at different levels of the mesocorticolimbic circuits may underlie the insensitivity to cocaine reinforcing properties in these mice. Therefore, we decided to characterize the contribution to cocaine addictive properties of *Maged1* expression in key neuronal populations of the mesocorticolimbic system using cell-specific gene inactivation tools.

Midbrain DA neurons are well recognized as the principal target neurons of cocaine. In order to understand the role of *Maged1* in the physiology of DA neurons, we generated a conditional knockout model by crossing *Maged1* floxed mice (*Maged1*^{LoxP} [21]) with mice expressing Cre-recombinase specifically in DA neurons (*DATCre* mice [33]). *In situ* hybridization analysis showed a selective reduction of *Maged1* mRNA in midbrain nuclei of *DATCre*-positive *Maged1*^{LoxP} mice with no change in tyrosine hydroxylase (TH) mRNA

expression levels (Fig 4A and B). Behavioural testing showed that loss of *Maged1* in DA cells affected neither spontaneous locomotor activity in an open-field arena nor motor coordination in the accelerated rotarod test (Fig 4C and D). Acute cocaine injection (20 mg/kg, ip) induced a similar increase in locomotion in Cre-positive and Cre-negative *Maged1*^{LoxP} mice; however, *DATCre* *Maged1*^{LoxP} mice displayed an unexpected increase in the locomotor response to cocaine that saturated after the 2nd day of administration, as compared to their control littermates (Fig 4E). Similar to *Maged1*^{KO} mice, the effect of bath cocaine application on DA release evoked in the striatum was similar in slices prepared from *DATCre* *Maged1*^{LoxP} mice and from control mice indicating that cocaine-mediated DA uptake inhibition is preserved in these mice (Fig EV4). As mice with the conditional deletion of *Maged1* in DA neurons did not recapitulate the phenotypes observed in constitutive *Maged1*^{KO} mice, we concluded that *Maged1* in DA cells is not responsible for insensitivity to cocaine-elicited motor effects observed in constitutive *Maged1*^{KO} mice.

Striatal neurons are the principal target of midbrain DA pathway. We thus deleted *Maged1* specifically in the striatum. This was

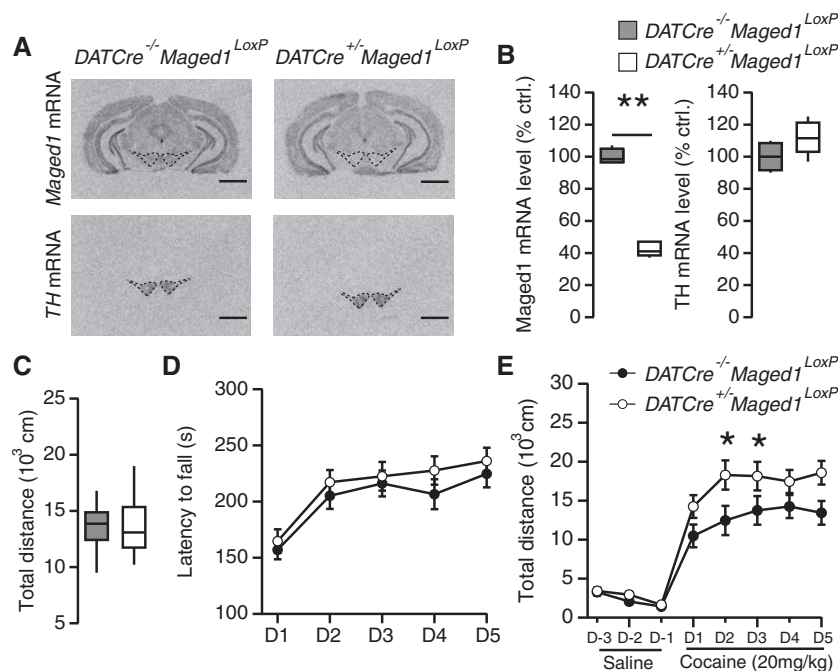


Figure 4. Conditional knockout of *Maged1* in DA neurons.

- A *In situ* hybridization autoradiograms of *Maged1* and TH mRNA performed on coronal brain sections from *DATCre*-negative and *DATCre*-positive *Maged1*^{LoxP} mice. TH mRNA labelling was used to anatomically localize midbrain nuclei containing DA neurons (scale bar: 1 mm).
- B Quantification of optical densities revealed a significant decrease in *Maged1* expression in *DATCre*-positive *Maged1*^{LoxP} mice ($n_{\text{Cre-negative}} = 4$ mice, $n_{\text{Cre-positive}} = 6$ mice, $**P_{\text{Maged1}} = 0.0095$, $P_{\text{TH}} = 0.17$, Mann-Whitney *U* test).
- C Total distance travelled by *DATCre*-negative and *DATCre*-positive *Maged1*^{LoxP} mice during 1 h spent in an open-field arena ($n_{\text{Cre-negative}} = 12$ mice, $n_{\text{Cre-positive}} = 16$ mice, $P = 0.35$, Mann-Whitney *U* test).
- D Motor coordination and motor skills learning as scored as the latency to fall from an accelerating rotarod (mean \pm s.e.m., $n_{\text{Cre-negative}} = 12$ mice, $n_{\text{Cre-positive}} = 16$ mice, *DATCre*-negative versus *DATCre*-positive *Maged1*^{LoxP}, $P = 0.43$; time, $P < 0.0001$; interaction factor, $P = 0.95$, repeated-measures two-way ANOVA).
- E Locomotor response to daily injections of cocaine (20 mg/kg, ip, mean \pm s.e.m., $n_{\text{Cre-negative}} = 11$ mice, $n_{\text{Cre-positive}} = 15$ mice, *DATCre*-negative versus *DATCre*-positive *Maged1*^{LoxP}, $P = 0.0276$; time, $P < 0.0001$; interaction factor, $P = 0.0139$, repeated-measures two-way ANOVA; * $P < 0.05$ as compared to *DATCre*-negative, Sidak's post-test).

Data information: Boxplots represent median, first and third quartiles, whiskers indicating the maximal and minimal values observed.

performed by crossing *Maged1^{LoxP}* mice with mice expressing Cre-recombinase under the transcriptional control of the intergenic region of *Distal-less homeobox 5/6* (*Dlx5/6* [34]). *Maged1* mRNA expression was greatly reduced in the striatum following Cre-mediated knockout as measured by *in situ* hybridization (Fig 5A and B). There was also a reduction in *Maged1* expression in the motor cortex, likely due to the expression of *Dlx5/6* in cortical interneurons. Thus, Cre-recombinase expression can be driven by the intergenic region of *Dlx5/6* reliably to induce the recombination of the *Maged1* conditioned allele. However, loss of *Maged1* in striatal neurons affected neither spontaneous locomotor activity nor motor coordination (Fig 5C and D).

In addition to GABAergic projection neurons of the striatum, other inhibitory neurons, such as those of the VTA, can modulate behavioural responses to drugs of abuse such as cocaine

and nicotine [35,36]. To delete *Maged1* in GABAergic neurons, *Maged1^{LoxP}* mice were crossed with mice expressing Cre-recombinase under the control of the glutamate decarboxylase gene (*Gad2*) promoter [37]. The *Maged1* mRNA was virtually undetectable in the striatal region of slices from *Gad2^{Cre/wt} Maged1^{LoxP}* mice (Fig 5E and F). As in *Dlx5/6Cre^{+/-} Maged1^{LoxP}* mice, we observed a reduction in *Maged1* mRNA levels in the cortex. The expression of the *Maged1* mRNA was also reduced by 35% in midbrain nuclei containing DA neurons, consistent with the proportion of GABAergic neurons previously reported in these brain regions [38]. Despite effective deletion of the *Maged1* floxed allele in GABAergic neurons, *Gad2^{Cre/wt} Maged1^{LoxP}* mice showed normal cocaine-induced locomotor sensitization when compared to control animals (20 mg/kg, ip; Fig 5G). Thus, conditional deletion of *Maged1* in the striatum or in GABAergic

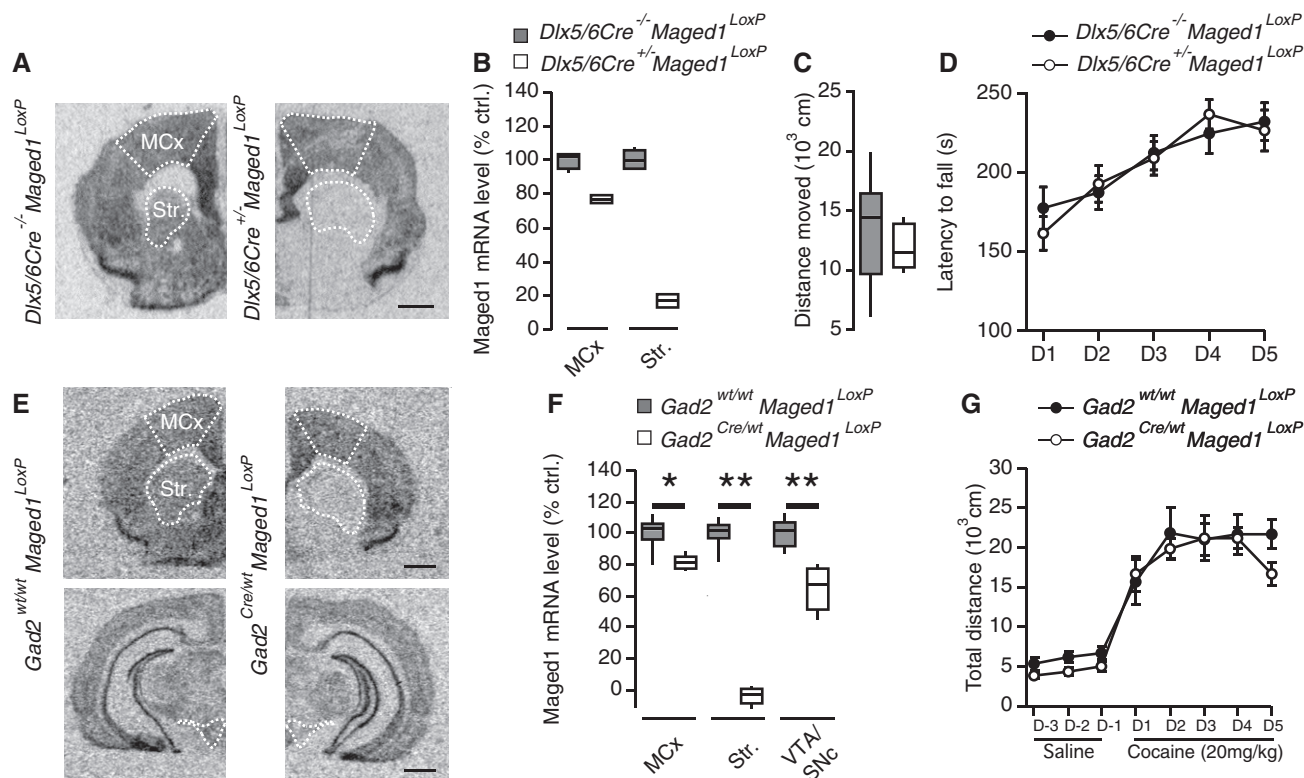


Figure 5. Conditional knockout of *Maged1* in striatal neurons.

- A *In situ* hybridization autoradiograms of *Maged1* mRNA performed on coronal brain sections from *Dlx5/6Cre*-negative and *Dlx5/6Cre*-positive *Maged1^{LoxP}* mice (scale bar: 1 mm).
- B Quantification of optical densities in the motor cortex (MCx) and the striatum (Str.; $n_{\text{Cre-negative}} = 4$ mice, $n_{\text{Cre-positive}} = 2$ mice).
- C Total distance travelled by *Dlx5/6Cre*-negative and *Dlx5/6Cre*-positive *Maged1^{LoxP}* mice during 1 h spent in an open-field arena ($n_{\text{Cre-negative}} = 8$ mice, $n_{\text{Cre-positive}} = 6$ mice, $P = 0.47$, Mann–Whitney *U* test).
- D Motor coordination and motor skills learning as scored as the latency to fall from an accelerating rotarod (mean \pm s.e.m., $n_{\text{Cre-negative}} = 8$ mice, $n_{\text{Cre-positive}} = 6$ mice, *Dlx5/6Cre*-negative versus *Dlx5/6Cre*-positive *Maged1^{LoxP}*, $P = 0.84$; time, $P < 0.0001$; interaction factor, $P = 0.53$, repeated-measures two-way ANOVA).
- E *In situ* hybridization autoradiograms of *Maged1* mRNA performed on coronal brain sections from *Gad2Cre*-negative and *Gad2Cre*-positive *Maged1^{LoxP}* mice (scale bar: 1 mm).
- F Quantification of optical densities in the MCx, the Str. and in the VTA and the *substantia nigra pars compacta* (SNc; $n_{\text{Cre-negative}} = 7$ mice, $n_{\text{Cre-positive}} = 6$ mice, $*P_{\text{MCx}} = 0.014$; $**P_{\text{Str.}} = 0.0012$, $**P_{\text{VTA/SNc}} = 0.0025$, Mann–Whitney *U* test).
- G Locomotor sensitization to cocaine (20 mg/kg, ip; mean \pm SEM, $n_{\text{Cre-negative}} = 11$ mice, $n_{\text{Cre-positive}} = 6$ mice, *Gad2Cre*-negative versus *Gad2Cre*-positive *Maged1^{LoxP}*, $P = 0.71$; time, $P < 0.0001$; interaction factor, $P = 0.53$, repeated-measures two-way ANOVA).

Data information: Boxplots represent median, first and third quartiles, whiskers indicating the maximal and minimal values observed.

neurons throughout the brain did not recapitulate the behavioural phenotype observed in constitutive *Maged1*^{KO} mice. Therefore, *Maged1* expression in GABA neurons is not necessary for the baseline motor behaviour or for locomotor stimulating effects of cocaine.

Requirement of *Maged1* in the PFC and the amygdala for cocaine sensitization

Prefrontal cortex is a major target of the mesocorticolimbic DA system and the origin of a main glutamatergic input to the NAc (see above). We achieved the conditional deletion of *Maged1* in the PFC by stereotaxic injection of an adeno-associated virus carrying the coding sequence for Cre fused to eGFP (AAV-eGFP-Cre) into cortical regions of *Maged1*^{LoxP} mice. There was an 87% reduction of *Maged1* mRNA expression in the PFC of *Maged1*^{LoxP} mice injected with AAV-eGFP-Cre without any observable neurotoxic effect of this acute *Maged1* deletion (Figs 6A and B and EV5). Mice lacking *Maged1* in the PFC showed normal baseline locomotion, as measured by total distance travelled over 1 h in an open field (Fig 6C), as well as normal motor coordination on the first day of rotarod testing. However, mice lacking *Maged1* specifically in the PFC improved their performance on the rotarod much more slowly than control mice (Fig 6D). Similarly, acute injection of cocaine (20 mg/kg, ip) resulted in a normal increase in locomotor activity in these mice. Repeated daily cocaine injections resulted in locomotor sensitization in both groups. However, locomotor sensitization was significantly attenuated in mice lacking *Maged1* in the PFC (Fig 6E). This suggests that expression of *Maged1* in the PFC is necessary for the ability of mice to alter their behavioural responses over time. In contrast to the impairment in locomotor responses to chronic cocaine administration, AAV-Cre injected *Maged1*^{LoxP} mice showed a normal preference for the cocaine-paired

compartment in the CPP paradigm (Fig 6F). Thus, mice lacking *Maged1* in the PFC partially recapitulate the phenotype displayed by mice with constitutive deletion of *Maged1*, suggesting that expression of *Maged1* in PFC is required for motor learning and locomotor sensitization to cocaine, but not for cocaine-induced reward in the CPP paradigm.

In mice lacking *Maged1* constitutively, the lack of behavioural response to cocaine was associated with impaired cocaine-induced DA increases in the NAc. As we observed a decrease in locomotor sensitization to cocaine in mice lacking *Maged1* in PFC, we also measured cocaine-induced DA changes in the NAc of these mice by *in vivo* microdialysis. Mice were implanted with microdialysis probes after 4 days of daily cocaine treatment (20 mg/kg, ip) to induce locomotor sensitization. On the fifth day, a significant decrease in basal DA concentration was observed in the NAc of mice lacking *Maged1* in the PFC as compared to control animals (Fig 6G). Moreover, the ability of cocaine to increase extracellular DA concentration was also attenuated in these mice (Fig 6G), demonstrating that *Maged1* expression in the PFC is important for neurochemical and behavioural sensitization to cocaine.

The amygdala provides with the PFC a convergent glutamatergic input to the NAc and is involved in addictive processes [39,40]. Therefore, we performed the deletion of *Maged1* in the amygdala following the same strategy as for the PFC (Fig 6H and I). This manipulation did not affect locomotion or motor coordination (Fig 6J and K). However, contrary to what we observed after the deletion of *Maged1* in the PFC, its inactivation in the amygdala did not induce a defect in motor learning (Fig 6K). The effect of cocaine administration (20 mg/kg, ip) on locomotor activity also contrasted with the PFC experiments. Here, we observed a strong reduction in the acute effect of cocaine whereas a sensitization took place over time (Fig 6L).

Figure 6. Conditional knockout of *Maged1* in the PFC and the amygdala.

- A *In situ* hybridization autoradiograms of *Maged1* mRNA from *Maged1*^{LoxP} mice bilaterally injected with AAV-eGFP or AAV-eGFP-Cre in the PFC (scale bar: 1 mm).
- B Quantification of optical densities in infralimbic (IL) and prelimbic (PrL) areas of the PFC ($n_{\text{eGFP}} = 13$ mice, $n_{\text{Cre}} = 14$ mice, $P < 0.0001$, Mann–Whitney *U* test).
- C Locomotor activity of AAV-eGFP or AAV-eGFP-Cre injected *Maged1*^{LoxP} mice in an open field ($n_{\text{eGFP}} = 13$ mice, $n_{\text{Cre}} = 14$ mice, $P = 0.17$, Mann–Whitney *U* test).
- D Motor coordination and motor skills learning as scored as the latency to fall from an accelerating rotarod (mean \pm s.e.m., $n_{\text{eGFP}} = 13$ mice, $n_{\text{Cre}} = 14$ mice, AAV-eGFP versus AAV-eGFP-Cre injected *Maged1*^{LoxP}, $P = 0.0127$; time, $P < 0.0001$; interaction factor, $P = 0.0268$, repeated-measures two-way ANOVA, Sidak's post-test).
- E Locomotor sensitization to cocaine (20 mg/kg, ip, mean \pm s.e.m., $n_{\text{eGFP}} = 13$ mice, $n_{\text{Cre, Sal.}} = 11$ mice, $n_{\text{Cre, Coc.}} = 14$ mice, AAV-eGFP versus AAV-eGFP-Cre injected *Maged1*^{LoxP}, $P = 0.0274$; time, $P < 0.0001$; interaction factor, $P = 0.002$, repeated-measures two-way ANOVA, Sidak's post-test).
- F CPP for cocaine (20 mg/kg, ip, mean \pm s.e.m., $n_{\text{eGFP, Sal.}} = 9$ mice, $n_{\text{eGFP, Coc.}} = 9$ mice, $n_{\text{Cre}} = 14$ mice, AAV-eGFP versus AAV-eGFP-Cre injected *Maged1*^{LoxP} $P = 0.23$; treatment, $P = 0.0011$; interaction factor, $P = 0.27$, two-way ANOVA).
- G After recovery from AAV injection surgery, mice were treated for 4 days with cocaine (20 mg/kg, ip) and implanted with a microdialysis probe in their NAc. Extracellular DA concentration was assessed in basal conditions ($n_{\text{eGFP}} = 9$ mice, $n_{\text{Cre}} = 8$ mice, $P = 0.0102$, Mann–Whitney *U* test) and after cocaine injection (20 mg/kg, ip, mean \pm s.e.m., AAV-eGFP versus AAV-eGFP-Cre injected *Maged1*^{LoxP}, $P = 0.0007$; time, $P < 0.0001$; interaction factor, $P = 0.0001$, repeated-measures two-way ANOVA, Sidak's post-test).
- H *In situ* hybridization autoradiograms of *Maged1* mRNA from *Maged1*^{LoxP} mice bilaterally injected with AAV-eGFP or AAV-eGFP-Cre in the amygdala (Amg) (scale bar: 1 mm).
- I Quantification of optical densities ($n_{\text{eGFP}} = 10$ mice, $n_{\text{Cre}} = 9$ mice, $P < 0.0001$, Mann–Whitney *U* test).
- J Locomotor activity of AAV-eGFP or AAV-eGFP-Cre injected *Maged1*^{LoxP} mice in an open field ($n_{\text{eGFP}} = 10$ mice, $n_{\text{Cre}} = 9$ mice, $P = 0.14$, Mann–Whitney *U* test).
- K Motor coordination and motor skills learning scored as the latency to fall from an accelerating rotarod ($n_{\text{eGFP}} = 10$ mice, $n_{\text{Cre}} = 9$ mice, mean \pm s.e.m., AAV-eGFP versus AAV-eGFP-Cre injected *Maged1*^{LoxP}, $P = 0.72$; time, $P < 0.0001$; interaction factor, $P = 0.29$, repeated-measures two-way ANOVA).
- L Locomotor sensitization to cocaine (20 mg/kg, ip, $n_{\text{eGFP}} = 10$ mice, $n_{\text{Cre}} = 8$ mice, mean \pm s.e.m., AAV-eGFP versus AAV-eGFP-Cre injected *Maged1*^{LoxP}, $P = 0.0011$; time, $P < 0.0001$; interaction factor, $P = 0.0018$, repeated-measures two-way ANOVA; Sidak's post-test).
- M Cocaine self-administration ($n_{\text{eGFP}} = 7$, $n_{\text{Cre, PFC}} = 7$, $n_{\text{Cre, Amg}} = 7$, $n_{\text{Cre, PFC \& Amg}} = 6$ mice, mean \pm s.e.m., 1 mg/kg/infusion; time, $P < 0.0001$; time \times group, $P = 0.079$; time \times active/inactive, $P < 0.0001$; time \times group \times active/inactive, $P = 0.912$ repeated-measures three-way ANOVA). Dashed lines with triangles represent data measured from inactive holes of the apparatus.

Data information: Boxplots represent median, first and third quartiles, whiskers indicating the maximal and minimal values observed. * $P < 0.05$, ** $P < 0.01$, *** $P < 0.001$.

Given these two distinct effects of the deletion of *Maged1* in two different regions of the mouse brain, we tested the reinforcing effect of cocaine on both deletion models in a self-administration paradigm. However, neither mice with *Maged1* deletion in PFC, nor those with deletion in amygdala showed any significant alteration in the ability to self-administer cocaine (Fig 6M). An additional group of animals was injected with AAV-eGFP-Cre vectors in both

structures in order to assess a potential combinatory effect. These mice were also able to self-administer normally (Fig 6M). Therefore, it appears that the expression of *Maged1* in adult mouse PFC and amygdala specifically modulates locomotor sensitization to cocaine. In addition, *Maged1* affects the kinetics of sensitization acquisition via glutamatergic afferents in a region-dependent manner.

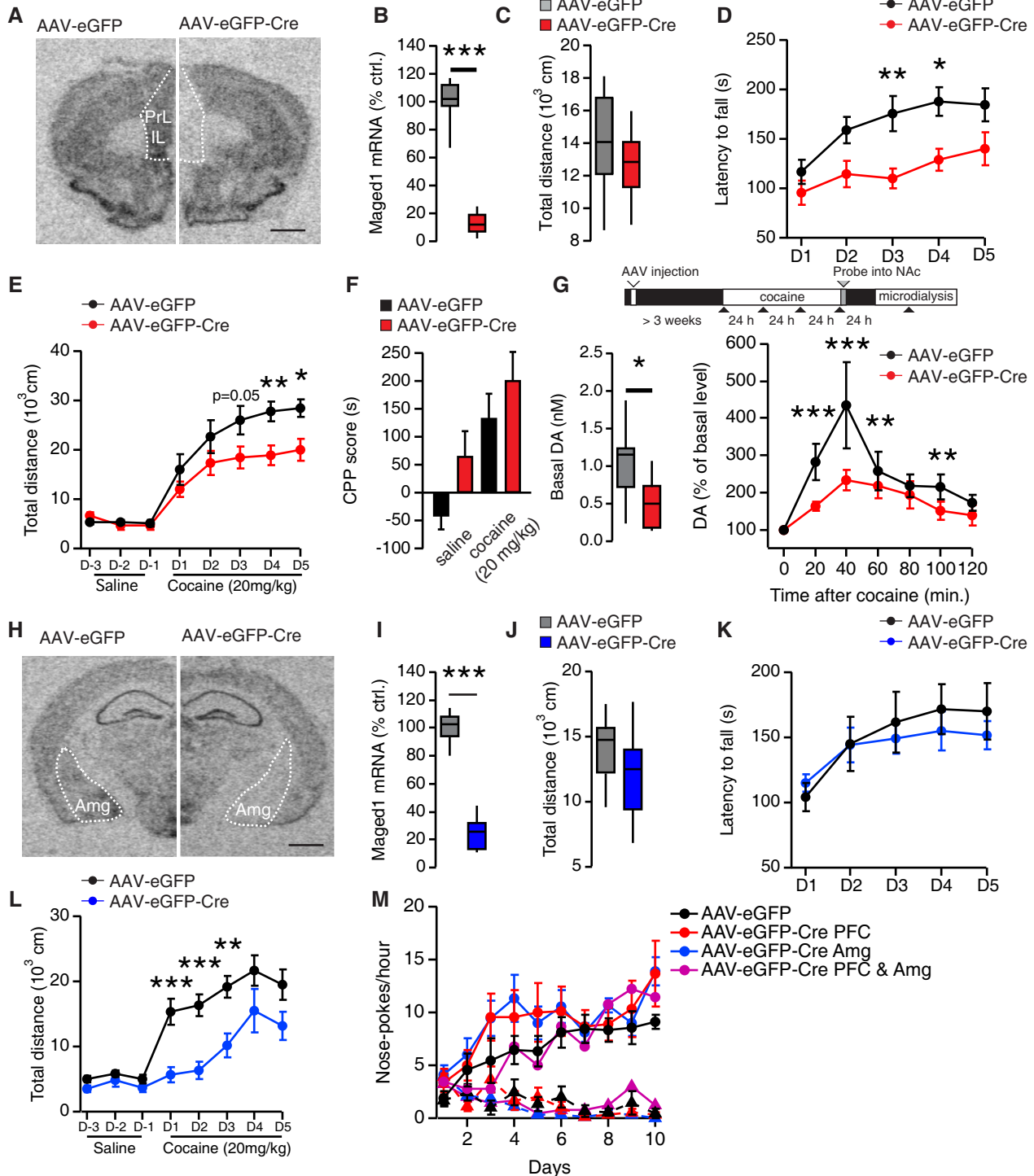


Figure 6.

Discussion

Maged1 regulates a large variety of behaviours and has been implicated in psychiatric disorders. Here, we show that the *Maged1* gene is involved in motor behaviours and is essential for behavioural responses to cocaine. Mice lacking *Maged1* constitutively were completely unresponsive to cocaine in behavioural models of addiction in rodents, including locomotor sensitization, CPP and self-administration. As drugs of abuse act on the mesocorticolimbic system, we studied the role of *Maged1* in different regions of this circuit.

Within the mesocorticolimbic system, the NAc integrates afferents from many brain areas, including glutamatergic projections from the PFC, the amygdala and the hippocampus, and dopaminergic inputs from the VTA. Many studies have demonstrated the importance of glutamatergic transmission in the NAc for the development and persistence of behaviours related to addiction [8,9,28,41]. Using whole-cell recordings in acute brain slices, we show that glutamatergic transmission is altered in the NAc of mice lacking *Maged1* constitutively as demonstrated by a decrease in A/N ratio at cortico-accumbal synapses. This is reminiscent of observations in cocaine-treated mice after 1–2 days of abstinence [5,32]. In cocaine-treated mice, the decrease in A/N ratio is thought to be related to depression of cortico-accumbal synapses due to the internalization of AMPA-Rs [7]. In *Maged1*-deficient mice, the decrease in A/N ratio is not associated with changes in mEPSC amplitude or frequency, usually used as markers of synaptic strength. However, our mEPSC analysis was limited by the multiplicity of the glutamatergic inputs converging on the NAc [6]. Indeed, evoked EPSCs can result from activation of distinct sets of AMPA-Rs [42]. However, mEPSCs recorded in slices prepared from *Maged1*^{KO} mice were slower than those from wild-type mice. This has also been observed in the NAc of rats that self-administered cocaine, again after a short withdrawal period [43]. Finally, cortico-accumbal glutamatergic synapses of cocaine-addicted mice and those of *Maged1*-deficient mice are also similarly resistant to the induction of LTD [8,9]. This form of plasticity is of particular behavioural relevance given that its impairment prevents the expression of sensitization to psychostimulants [7].

Plasticity at glutamatergic synapses in the NAc can involve either post- or presynaptic mechanisms [29]. Thus, we targeted deletion of *Maged1* specifically to the post-synaptic (the NAc) or presynaptic (the PFC) cell populations of the cortico-accumbal pathway using the Cre/LoxP system. Deletion of *Maged1* in the striatum did not induce any alteration in the behaviours examined. In contrast, deletion of *Maged1* in the PFC partially recapitulated the behavioural phenotype observed in mice with constitutive deletion. Interestingly, the complete lack of *Maged1* impaired motor coordination but did not affect motor learning, whereas deletion of *Maged1* only in the PFC resulted in no alteration of motor coordination, but in a severe deficit in motor learning. This latter phenotype is consistent with the function of PFC projections to the dorso-medial striatum [44], which are known to regulate the initial phase of motor skills acquisition [45]. Deletion of *Maged1* in the PFC also did not reproduce the complete insensitivity to cocaine observed in constitutive knockout mice but produced a decrease in sensitization, again in accordance with the role of the PFC in the expression of behavioural sensitization [46]. Although the PFC is also involved in CPP acquisition and self-administration [9,47], we did not see any effect of

Maged1 deletion in PFC on cocaine CPP or self-administration. Such a decoupling between locomotor sensitization and CPP has been reported for other knockout models, such as mice lacking calcium/calmodulin protein kinase II α , a protein involved in synaptic plasticity [48], suggesting that these behavioural responses to cocaine are driven by different mechanisms.

A further reason for the partial discrepancy between the behavioural phenotype of mice with adult *Maged1* deletion in PFC and amygdala and constitutive *Maged1* knockout may be a role of this gene in the development of these structures. Indeed, *Maged1* is expressed in the brain during mouse development from embryonic day E7 [49] and is involved in processes such as neuronal apoptosis, differentiation and migration [21,50]. Our constitutive knockout model might therefore suffer from developmental defects contributing to the observed phenotypes. The impairments observed following deletion of *Maged1* in the PFC or the amygdala in adult mice also show that *Maged1* plays a specific role in adult brain physiology, independent from developmental processes. In contrast, deletion of *Maged1* in the striatum was achieved using a Cre-recombinase (driven by the intergenic region of *Dlx5/6*) which is expressed between E8.5 [51] and E12.5 [52] and by the promoter of *Gad2* which is expressed from E10.5 [53], suggesting that the ablation of the *Maged1* locus in the striatum and GABAergic neurons in these mice occurs at least 2 days after the onset of *Maged1* expression. However, these genetic manipulations did not induce any behavioural phenotype. This could be explained by a compensatory effect exerted by other components of the network or by an absence of behaviourally relevant function for *Maged1* in these neurons.

In addition, the phenotypes observed in PFC or amygdala injected mice could be due to a defect in glutamatergic transmission and/or to alterations in GABAergic interneuron functions, since stereotaxic injections of AAVs do not distinguish between different neuronal populations. *Dlx5*, -6 and *Gad2* are both expressed in cortical and amygdalar GABAergic neurons [54]. The observed decrease in *Maged1* mRNA levels in the cortex of *Dlx5/6Cre Maged1*^{LoxP} and *Gad2Cre* mice is, indeed, consistent with a lack of expression of *Maged1* in cortical interneurons. Notably, both *Dlx5/6Cre* and *Gad2Cre Maged1*^{LoxP} mice did not show any behavioural defects, thus suggesting that cortical and amygdalar GABAergic neurons are probably not involved in the behavioural functions of *Maged1* studied here. Alternatively, the inactivation of *Maged1* in both glutamatergic and GABAergic neuronal populations might be required to alter the functions of cortical and amygdalar networks and their glutamatergic output. Taken together, our results thus suggest that the function of *Maged1* in the mesocorticolimbic circuit most likely results from the complex interplay between *Maged1* developmental functions and the combination of its different activities in the different components of the network.

In addition to an impairment in glutamatergic transmission, we identified alterations of DA transmission, in particular cocaine-elicited extracellular DA increase, in *Maged1*^{KO} mice. Mouri *et al* [17] found that *Maged1*^{KO} mice display similar deficits in serotonin transmission, another monoaminergic neurotransmitter. The decrease in extracellular serotonin measured *in vivo* was linked to enhanced uptake [17]. As we did not observe any difference in DAT expression or function, it seems likely that *Maged1* acts on the DA system in a different way than on the serotonin system. Moreover, bath application of cocaine on brain slices is able to induce

extracellular DA increase in *Maged1*^{KO} mice while this is not the case *in vivo*. This shows that direct molecular effects of cocaine are preserved in *Maged1*^{KO} mice. Finally, mice lacking *Maged1* only in DA neurons did not recapitulate the phenotypes observed in constitutive knockout mice. They even show a paradoxical increase in the locomotor effect of cocaine, suggesting that *Maged1* exerts a function in DA neurons, during their development and/or in the adult animal that is masked in the constitutive knockout. This function should, however, be different from the ones *Maged1* plays in the adult PFC or the amygdala. Taken together, our results suggest that *Maged1* acts indirectly on DA transmission. We propose that this indirect effect is mediated through glutamatergic neurons in the PFC, since the reduced cocaine sensitization in mice lacking *Maged1* in the PFC is accompanied by a reduction in cocaine-evoked DA increase. Recent evidence shows that the PFC exerts control over the DA transmission in the striatum by regulating the firing of DA neurons in the VTA [55,56]. In our case, DA neurons showed normal electrophysiological properties in anesthetized *Maged1*^{KO} mice, as well as normal basal DA levels. However, we cannot exclude that DA neurons behave differently in awake animals. In addition, studies in brains slices have shown that glutamate regulates DA release in the striatum [57]. Other studies indicate that PFC fibre stimulation in the NAc can induce DA release [58,59]. In addition, low-frequency stimulation of these axons has been showed to revert cocaine sensitization [8]. Therefore, our results support the hypothesis that *Maged1* regulates DA transmission through its action on glutamatergic neurons of the PFC.

In mice, the identification of a gene whose ablation induces a complete lack of behavioural response to cocaine remains exceptional in the literature. To our best knowledge, the other examples are the DAT, the direct molecular target of cocaine [11], and mGluR5, another established component of the synaptic transmission machinery [60]. Therefore, the phenotypes described in this work identify *Maged1* as an essential molecule for behavioural responses to cocaine. Using site-specific conditional knockouts, we then dissected the neuronal network that might account for these phenotypes. We showed that the deletion of *Maged1* in the PFC or in the amygdala selectively disrupts motor learning and/or behavioural sensitization to cocaine while deletions in the striatal or DA neurons did not. However, none of these genetic manipulations fully recapitulated the phenotypes observed in the constitutive knockout model. This suggests that the function of *Maged1* in the mesocorticolimbic circuit, a primary target of drugs of abuse, most likely results from the complex interplay between *Maged1* developmental functions and the combination of its different activities in the different components of the network. This is consistent with the suggested role for *Maged1* as a scaffold protein whose functions are to bring together different effector proteins. Therefore, we hypothesize that the identification of *Maged1* molecular partners will shed light on the cellular mechanisms underlying drug addiction.

Materials and Methods

Animals

The *Maged1*-deficient (*Maged1*^{KO}) and conditioned (*Maged1*^{LoxP}) mice used in the present study have been previously described [21].

Maged1 knockout mice do not show gross abnormalities and have normal general cognitive and sensori-motor abilities [15,17]. They grow slightly slower than wild-type mice but reach normal weight after 4 weeks and also develop obesity after ~6 months [15]. Therefore, all our experiments were performed in 1- to 6-month-old mice. As the *Maged1* locus is located on the X chromosome, our experiments were conducted on hemizygous *Maged1*^{KO} males and their wild-type littermates (*Maged1*^{WT}) generated by crossing heterozygous *Maged1*^{KO/WT} females with C57Bl6J males. Conditional knockout mice were generated by crossing heterozygous *Maged1*^{LoxP/WT} or homozygous *Maged1*^{LoxP/LoxP} females with different population-selective Cre male mice. The Cre-mediated deletion of *Maged1* was obtained using mice expressing Cre-recombinase under the control of the *Slc6a3* promoter (*DATCre* mice [33]), the intergenic region of *Dlx5/6* genes (*Dlx5/6Cre* mice [34,61]) and the *Gad2* promoter (*Gad2*^{Cre/WT} mice [37]). All mice were backcrossed for at least eight generations in the C57Bl6J genetic background. Mice were housed by groups of 3–5 mice, in a 12 h light/dark cycle, with food and water available *ad libitum*. Experimental procedures were performed in accordance with the Institutional Animal Care Committee guidelines and approved by the local ethics committees.

AAV stereotaxic injections

Nine to twelve weeks old *Maged1*^{LoxP} mice were anaesthetized with avertin (2,2,2-tribromoethanol 1.25%; 2-methyl-2-butanol 0.78%, 20 µl/g, ip, Sigma-Aldrich) before bilateral injection with a serotype 1 adeno-associated virus (AAV) solution into the PFC and/or the amygdala using the following stereotaxic coordinates (from bregma, in mm): PFC, A-P 1.9, M-L ±0.3, D-V -2.3; amygdala, A-P -0.1, M-L ±3.0, D-V -4.9. AAVs containing the Cre-recombinase coding sequence fused with eGFP (AAV-eGFP-Cre) or eGFP only as a control (AAV-eGFP) were injected at a volume of 600 nl per side. AAV vectors were purchased from Penn Vector Core. To avoid bias, littermates were equally distributed between the two groups. After surgery, mice were allowed to recover for at least 3 weeks.

Behavioural analysis

Two- to 6-month-old mice were used for behavioural testing. Experiments were performed during the light period of the cycle.

Open field

Mice were tested in a squared open-field arena (40 × 40 cm, 30 cm high) made of grey (wall) and white (floor) hard plastic. Locomotor activity was recorded with a video camera placed on the ceiling above the arena and connected to an automated video tracking system (Ethovision XT, Noldus Information Technology). Spontaneous locomotor activity was measured as total distance travelled (in cm) during 60 min in a low luminosity environment (15–20 lx).

Accelerated rotarod

The rotarod apparatus consisted of a rotating rod (diameter 3 cm; hard non slipping plastic) divided into five 5 cm lanes (Ugo-Basile). The day before starting experiment, mice were trained on the apparatus until the animals were able to stay on the rod rotating at a constant speed of 4 rpm for 60 s. For testing, mice were placed individually for four consecutive trials per day (1 h inter-trial intervals)

on the rod rotating at an accelerating speed from 4 to 40 rpm in 300 s. The latency to fall off the rod was recorded. Mice staying on the rod more than 300 s were removed from the apparatus and scored at 300 s.

Locomotor sensitization

Animals were allowed to freely explore the recording chambers for 30 min (20 cm × 40 cm; 30 cm high). In the three-first days of experiment, mice were injected with saline and their locomotor activity was recorded during 1 h (Ethovision XT). In the next 5 days, mice were injected with cocaine instead of saline (20 mg/kg, i.p.).

Conditioned place preference (CPP)

Conditioned place preference was conducted in a three chambers apparatus, consisting of a small middle neutral (6 × 20 cm) area connected to two large compartments (18 × 20 cm) that differed in wall and floor conditions (Panlab). Three days before the experiment, mice were used to be manipulated and received a single saline injection in their home cage. At day 0 (preconditioning test, 18 min), mice were placed in the central neutral area and allowed to explore freely both chambers. Mice were randomly assigned to the various experimental groups (unbiased protocol). Conditioning (days 1–6) was carried out as follows: mice were confined to one compartment for 30 min immediately after injection of cocaine (20 mg/kg, ip, or saline for control groups) on days 1, 3 and 5 and to the other compartment after saline injection on days 2, 4 and 6. For the post-conditioning test (day 7), mice were placed in the central area and allowed to explore freely both chambers for 18 min. Results were expressed as the difference in time spent in the drug-paired compartment between post- and preconditioning tests.

Food and cocaine self-administration

The self-administration experiments were conducted in mouse operant chambers (Model ENV307A-CT, Medical Associates) equipped with two holes, one was selected as active hole for delivering the reinforcer and the other as inactive hole. Nose-poking on the active hole delivered a reinforcer (food pellet or cocaine infusion), while nose-poking on the inactive hole had no consequence. The chambers were housed in sound and light-attenuated boxes equipped with fans to provide ventilation and ambient noise. A removable food dispenser equidistant between the two nose-pokes permitted the delivery of food pellets when required. A stimulus light, located above the active hole, was paired contingently with the delivery of the reinforcer. The same operant chambers were used for drug self-administration, except that drinking and food dippers were removed.

Food-maintained behaviour Mice were food deprived (3.5 g of food was provided daily) during 4 days, in order to obtain 95% of their initial weight. The same food deprivation regime was maintained during the whole evaluation of food-maintained operant behaviour. Water was available *ad libitum* during this experimental phase. Four days after starting food deprivation, mice were trained in the operant chambers to nose-poke for food pellets (Noyes Precision Pellets, Research Diets Inc.). Self-administration sessions (1 h, daily) were conducted 6 days per week as

previously reported [62]. The house light was on at the beginning of the session for 3 s and off during all the session. First, mice were trained under an FR1 schedule of reinforcement. A 10 s time-out period was established after each reinforcement. During this 10 s period, the cue light was off and no reward was provided on the active hole. Responses on the inactive hole and all the responses during the 10 s time-out period were also recorded. The session was terminated after 100 reinforcers were delivered or after 1 h, whichever occurred first. The criteria for the acquisition were achieved when mice maintained a stable responding with less than 20% deviation from the mean of the total number of reinforcers earned in three consecutive sessions (80% of stability), with at least 75% responding on the active hole, and a minimum of 10 reinforcers per session. After each session, mice were returned to their home-cages.

Surgery for drug self-administration study Mice were anaesthetized under isoflurane anaesthesia (1.5–2.0%) and then implanted with indwelling intravenous catheters as previously described [62] with minor modifications. Briefly, a 6 cm length of tubing (0.3 mm inner diameter, 0.6 mm outer diameter, Silastics, Dow Corning) was fitted to a 22 gauge steel cannula (Semat) that was bent at a right angle and then embedded in a cement disc (Dentalon Plus) with an underlying nylon mesh. The catheter tubing was inserted 1.3 cm into the right jugular vein and anchored with suture. The remaining tubing ran subcutaneously to the cannula, which exited at the midscapular region. All incisions were sutured and coated with antibiotic ointment (Bactroban, GlaxoSmithKline). After surgery, animals were allowed to recover for 3 days prior to initiation of self-administration sessions. The patency of intravenous catheters was evaluated periodically (approximately every 6 days) and whenever drug self-administration behaviour appeared to deviate dramatically from that observed previously, by the infusion of 0.1 ml of thio-barbital (5 mg/ml) through the catheter. If prominent signs of anaesthesia were not apparent within 3 s of the infusion, the catheter was surgically removed, and a new catheter was implanted in the opposite jugular vein using the surgical procedure described above.

Drug self-administration procedure Cocaine self-administration sessions were conducted 3 days after surgery using the schedule described above for food self-administration with the following exceptions [62,63]. Responding was maintained by cocaine (1 mg/kg/injection) delivered in 23.5 µl over 2 s. Cocaine was infused via a syringe that was mounted on a microinfusion pump (PHM-100A, Med-Associates) and connected via Tygon tubing (0.96 mm outer diameter, Portex Fine Bore Polythene Tubing, Portex Ltd.) to a single-channel liquid swivel (375/25, Instech Laboratories) and to the mouse intravenous catheters. The swivel was mounted on a counterbalanced arm above the operant chamber. Mice were trained to nose-poke in order to receive a cocaine injection under an FR1 schedule of reinforcement. Self-administration sessions (1 h, daily) started with a priming injection of the drug. The number of reinforcers was limited to 50 infusions per session and each reinforcer was followed by a 30 s time-out period where active nose-poking had no consequence. The stimulus light signalled delivery of the reinforcer.

In vivo microdialysis

Two- to 6-month-old mice were anaesthetized with halothane (Fluothane) and placed in a flat skull position in a Kopf stereotaxic apparatus fitted with a mouse adapter. A microdialysis probe (CMA 7/2, 2 mm dialysis membrane, Carnegie Medicine) was inserted through a guide cannula into the right NAc at the following coordinates (from bregma, in mm): A-P = +1.5, M-L = -0.5, D-V = -5.2. The guide cannula was permanently secured with epoxy glue. After surgery, mice were placed in a circular Plexiglas cage and were allowed to recover overnight before the microdialysis experiment. The day after implantation, the inlet tubing of the probe was connected to a microinjection pump (CMA/100, Carnegie Medicine) and perfused with artificial cerebrospinal fluid (aCSF: KCl 2.5 mM, NaCl 125 mM, CaCl₂ 1.26 mM, MgCl₂ 1.18 mM, Na₂HPO₄ 2 mM, pH 7.4) at a flow rate of 1.1 µl/min (22 µl/20 min sample). 60 min later, four 20 min samples were collected to determine basal perfusate DA levels before cocaine (10 or 20 mg/kg, i.p.) injection. Six samples were collected after cocaine injection. At the end of the experiment, the brain was removed from the skull and the position of the microdialysis probe was verified.

A 20 µl volume from each sample was injected into an HPLC system with electrochemical detection for determination of DA concentration (ESA coulometric detector with a 5014 B cell, voltage: E₁ = -150 mV; E₂ = +220 mV (Coulchem II Electrochemical Detector). Separation of DA was performed on an ESA HR-80 column (80 × 4.6 mm I.D.). The mobile phase consisted of 18% methanol in 75 mM Na₂HPO₄, 1 mM 1-octanesulfonic acid and 20 mM EDTA (pH 5.6). The flow rate was 0.8 ml/min (Shimadzu LC-10ADVP, Solvent Delivery Module). The chromatograms were integrated using Jasco Borwin HPLC Software. DA detection limit was 5 fmol/sample.

In vivo extracellular recordings

Single-unit recordings of VTA DA cells were performed in 3- to 6-month-old anaesthetized mice as previously described [64,65]. Animals were deeply anaesthetized with chloral hydrate (400 mg/kg, ip), supplemented if required to maintain anaesthesia throughout experiment. Glass electrodes (6–9 MΩ) were pulled from borosilicate glass capillaries (Harvard Apparatus) and were filled with 0.5% sodium acetate. Electrodes were lowered in the central region of the VTA at the following stereotaxic coordinates (from bregma, in mm): A-P = -3 to -3.6, M-L = 0.4 to 0.5, D-V = -4 to -4.7. DA neurons were identified by mean of electrophysiological criteria: (i) firing rate between 1 and 10 Hz, (ii) typical triphasic action potential with a marked negative deflection, with a duration superior to 2 ms, and (iii) action potential width from beginning to negative trough superior to 1.1 ms. Following criteria were used to defined bursts of action potentials: a burst starts with a < 80 ms and ends with a > 160 ms inter-spike intervals [66]. In some experiments, cocaine (1 mg/kg) was intravenously injected through the left saphenous vein at least 5 min after the acquisition of spontaneous baseline activity. Those data are expressed as a percentage of the baseline firing frequency averaged during the 2 min before injection.

Acute brain slices preparation

Slices were prepared from 1- to 2-month-old mice. Mice were anaesthetized with halothane or isoflurane (LTD experiments) and sacrificed by decapitation. Brains were quickly removed and glued on the specimen disc of a vibratome (VT 1000S; Leica) and sliced in ice-cold choline-based aCSF: choline chloride 110 mM, KCl 2.5 mM, NaH₂PO₄ 1.25 mM, NaHCO₃ 25 mM, MgCl₂ 7 mM, CaCl₂ 0.5 mM and D-glucose 7 mM. Slices used for LTD experiments were prepared in ice-cold aCSF: NaCl 125 mM, KCl 2.5 mM, NaH₂PO₄ 1.25 mM, NaHCO₃ 25 mM, MgCl₂ 1 mM, CaCl₂ 2 mM, D-glucose 25 mM. Electrochemical detection of DA was performed in the dorsal striatum of coronal, 300 µm thick, slices. Intrinsic excitability of cortical neurons was assessed by recording of layer V/VI pyramidal cells in the IL/PrL regions of 220-µm-thick coronal slices. We recorded mEPSCs in the medial shell of the NAc of 220-µm-thick coronal slices. To evoke stimulated EPSCs in striatal projection neurons, we prepared 10° tilted parasagittal slices (300 µm thick) containing the PFC, the medial shell of the NAc and their connections [67]. After their preparation, slices were transferred into aCSF: NaCl 125 mM, KCl 2.5 mM, NaH₂PO₄ 1.25 mM, NaHCO₃ 26 mM, MgCl₂ 1 mM, CaCl₂ 2 mM and D-glucose 10 mM (25 mM for LTD experiments) and maintained at 34°C until use. Slices were allowed to recover at least 45 min before experiment. Solutions were continuously bubbled with 95% O₂, 5% CO₂. For experiments, slices were transferred into a recording chamber perfused with aCSF (1–2 ml/min), at room temperature.

Fast-scan cyclic voltammetry (FSCV)

Extracellular DA concentration in brain slices was monitored using FSCV with carbon fibre micro-electrodes (CFE) produced from 10 µm diameter carbon fibres (Cytec Carbon Fibres; tip length ~100 µm) pulled into borosilicate glass capillaries (Hilgenberg GmbH) using a two-stage vertical puller (PIP-5, HEKA Elektronik). CFE were placed into the dorsal striatum. Triangular voltage waves (-0.4 to 1.0 V versus Ag/AgCl; 300 V/s) were applied at a frequency of 10 Hz using an EPC-10 amplifier (HEKA Elektronik). Current traces were filtered using a low-pass Bessel filter set at 10 kHz, digitized at 25 kHz and acquired with the Patchmaster software (HEKA Elektronik). Background-subtracted cyclic voltammograms were analysed off-line using the IgorPro software (WaveMetrics). The oxidation peak current was converted into DA concentration by calibration of the electrode obtained in the recording chamber at the end of each experiment in 5 µM DA. DA overflow was evoked using a bipolar stimulating electrode (SNEX-200, Science Products GmbH) placed onto the striatum at ~100 µm from the recording electrode. A single-pulse stimulus (1 ms, 160 µA) was delivered every 3 min to allow complete recovery of the signal. Stimuli were generated by an Iso-Flex insulator (AMPI) driven by a pulse generator Master-8 (AMPI) triggered by the EPC-10 amplifier. A constant signal was generally obtained after three stimulations. After acquisition of ~10 DA transients, either cocaine or train of stimuli was applied. Cumulative concentrations of cocaine (0.1, 1.0 and 10 µM) were bath applied to the slice for 24 min each (8 stimulations). For another set of experiments, trains of five stimuli of increasing frequency (5, 10, 20 and 50 Hz) were applied. For single-pulse experiments, presented data are the averaged DA transients

obtained for eight consecutive stimulations (Fig 2E–G). For cocaine and multiple-pulse experiments, the three last consecutive traces were averaged for each condition (Figs EV1 and EV4).

Whole-cell recording in acute slices

Slices were visualized using a 40× water immersion objective (ACHROPLAN 40×/0.80 W, Carl Zeiss Instruments) of an upright microscope Axio Examiner A1 (Carl Zeiss Instruments) equipped with a CCD camera ORCA 05G (Hamamatsu Photonics). Patch pipettes (4–6 MΩ resistance) were pulled from borosilicate glass capillaries (Hilgenberg GmbH) using a two-stage vertical puller (PIP-5, HEKA Elektronik). Recordings were performed with an EPC-10 amplifier (HEKA Elektronik) driven by the Patchmaster software (HEKA Elektronik). Current traces were digitized at 10 kHz and on-line filtered at 3 kHz. Series resistance was monitored along experiments by a voltage step of –10 mV. Experiments with series resistance values > 35 MΩ (action potentials and EPSC) were discarded. LTD experiments were excluded if input resistance (R_i) varied by more than 20%. For action potentials and mEPSCs recording, the internal solution contained KMeSO₄ 125 mM, KCl 3 mM, CaCl₂ 0.022 mM, HEPES 10 mM, EGTA 0.1 mM, Na₂-phosphocreatine 5 mM, Mg-ATP 4 mM, Na₂-GTP 0.5 mM. For A/N ratio recordings, the internal solution contained CsCl 127 mM, CaCl₂ 0.022 mM, MgCl₂ 4 mM, HEPES 10 mM, EGTA 0.1 mM, Na₂-phosphocreatine 5 mM, K₂-ATP 4 mM, Na₂-GTP 0.5 mM, spermine 0.1 mM. For LTD experiments, the internal solution contained K-gluconate 122 mM, KCl 13 mM, HEPES 10 mM, EGTA 0.3 mM, Mg-ATP 4 mM, Na₂-GTP 0.3, Na-phosphocreatine 10 mM. Recordings were not corrected for liquid junction potentials. EPSCs were recorded in the presence of gabazine (SR-95531, 10 μM, Sigma-Aldrich). mEPSCs were recorded during 5 min at –70 mV in the presence of tetrodotoxin (TTX, 1 μM, Alomone labs). 457 ± 23 (*Maged1*^{WT}) and 462 ± 15 (*Maged1*^{KO}, mean ± s.e.m.) mEPSCs were analysed for each recorded cell. Evoked EPSCs in the NAc were obtained by single-pulse stimulations (0.2 ms, 600–1,000 μA, 0.1 Hz) delivered through a bipolar stimulating electrode (SNEX-200, Science Products GmbH) placed at the junction between the PFC and the NAc (A/N ratio) or in the layer 5 of the PFC (LTD). EPSCs were recorded at –70, 0 and +40 mV. L689,560 (10 μM, Tocris) was then added to block NMDA-R and isolate the AMPA-R component of EPSCs. NMDA-R-mediated currents were calculated off-line by subtracting the response at +40 mV in the presence of L689,560 from the response obtained in its absence. We computed AMPA-R_{–70 mV}/NMDA-R_{+40 mV} ratios by taking the averages of 10 EPSCs recorded in each condition. LTD was induced by the application of a low-frequency stimulation protocol: 1 Hz for 10 min. Data were analysed using Neuromatic (Jason Rothman, UCL, London, UK, <http://www.neuromatic.thinkrandom.com>) and SpAcAn (Guillaume P. Dugué & Charly Rousseau, ENS, Paris, France, <http://www.spacan.net>) packages for IgorPro (WaveMetrics).

In situ hybridization and receptor autoradiography

18-μm-thick coronal sections were prepared with a cryostat (CM 3050, Leica), mounted onto RNase-free glass-slides (SuperfrostPlus, Thermo Scientific) and stored at –20°C before experiment. *In situ* hybridization experiments were performed as previously described [68,69]. The sequences of the probes are provided in Table 1. After hybridization, the sections were covered with Carestream Biomax MR films (Perkin Elmer) for 1–2 weeks, depending on the mRNA studied. Autoradiograms were digitized at 256 grey levels using a CCD camera (Dage-MT1) driven by the 1.61 software (N.I.H. image), with fixed gain and black level. Averaged optical densities of manually defined areas of interest were computed with the ImageJ (N.I.H. image) software and background subtracted. Optical densities were averaged from 3 to 6 sections per area.

[¹²⁵I]RTI-55 was used as previously described to assess binding densities of the DAT [70,71]. Autoradiograms acquisitions and analysis were performed as described for *in situ* hybridization.

Immunohistochemistry

Mice bilaterally injected with AAV-eGFP-Cre (right hemisphere) and AAV-eGFP (left hemisphere) were transcardially perfused with a 0.01 M PBS solution followed by paraformaldehyde 4% in 0.1 M phosphate buffer (pH 7.4). Brains were removed, fixed overnight in paraformaldehyde 4% and successively cryoprotected in 20 and 30% sucrose in 0.1 M phosphate buffer. 20-μm-thick coronal sections were cut on a cryostat. Sections were incubated in 10% normal horse serum in 0.01 M PBS-0.1% Triton X-100 for 60 min at room temperature to block the nonspecific antibody binding. Sections were then incubated overnight at 4°C with the chicken anti-GFP antibody (1:2,000; ab13970; Abcam) in 1% normal horse serum, 0.01 M PBS and 0.1% Triton X-100. Antibody was then detected using a goat anti-chicken Alexa Fluor 488 (1:400; A11039; Invitrogen). Hoechst 33342 was used for nuclear staining (1:5,000; catalog #H3570; Invitrogen). Sections were mounted between slide and coverslip using FluorSave mounting medium (Calbiochem). Sections were imaged using an AxioImager Z1 (Zeiss) equipped with an objective a 20× Plan Apochromat 20×/0.8 NA. Excitation was provided by an HBO 105W lamp, and narrow bandpass filter sets (Zeiss) 49, 38 were used to visualize blue and green fluorochromes, respectively. Single plan images (1,388 by 1,040 pixels) were acquired with an AxioCam MRm (Zeiss) as 3 × 12 bit RGB proprietary *.zvi files (Zeiss), processed with AxioVision (4.6) software (Zeiss). Analysis was performed using Fiji software.

Statistics

Statistical analyses were performed using GraphPad Prism software (GraphPad Software Inc.). Threshold for significance was set at *P* < 0.05. Significance of two-sample comparisons was tested using

Table 1. Oligonucleotide probes sequences used for *in situ* hybridization.

| Probe | Sequence | Bases | cDNA | Reference |
|--------|----------------------------------------------------|-------------|-------|--------------------------|
| Maged1 | 5'-TCATACTCAGGAGGGTGTCTGTTGGCACTCGTCTATAGTCCAGG-3' | 2,051–2,095 | Mouse | * |
| TH | 5'-GGCCAGGGTGTGCAGCTCATCCTGGACCCCTCCAAGGACGCT-3' | 1,441–1,484 | Rat | Blum <i>et al</i> , 2004 |

*This paper.

two-sided Mann–Whitney *U* test. Those data are displayed as boxplots showing median, first and third quartiles, whiskers indicating the maximal and minimal values observed in the samples. Significance of repeated measures within an experimental group was tested using the Friedman test. Significance of multiple comparisons involving more than one variable was tested using two-way ANOVA followed by Tukey's or Sidak's *post hoc* tests. Repeated-measures tests were applied when appropriate. Those data are expressed as mean \pm s.e.m. For electrophysiology and FSCV experiments, sample sizes ("n") are given as the number of cells or slices/number of animals used for experiments. Otherwise, sample sizes are the number of animals.

Expanded View for this article is available online.

Acknowledgements

We thank M. Picciotto and M. Mameli for helpful comments and corrections on the manuscript, L. Cuvelier and D. Houtteman for expert technical assistance, S. Guiducci and N. Stasiak for contribution in microdialysis experiments and O. Carretón for her contribution in self-administration experiments. We thank F. Tronche (Université Pierre et Marie Curie, Paris, France) for providing *DATCre* mice; Dr. A. Goffinet and F. Tissir (Université Catholique de Louvain, Brussels, Belgium) for providing *Dlx5/6* cre mice and C. Lüscher (University of Geneva, Geneva, Switzerland) and G. Miesenböck (University of Oxford, Oxford, UK) for providing *Gad2^{Cre/WT}* mice. We are also grateful to F. Lemaître, M. Gilles, C. Amatore and J.-M. Kauffmann as well as Y. Schmitz, J.E. Lizardi-Ortiz and D. Sulzer for technical advices in fast-scan cyclic voltammetry. JFDB was supported by the Aspirant PhD fellowship from the FRS-FNRS and Van Buuren Funds, BD and AG are supported by the Aspirant PhD fellowship from the FRS-FNRS, JC was supported by a fellowship from the Fonds Erasme and SM was supported by a PhD fellowship from FRIA (Belgium) and a Biowin Program from the Walloon Region. AKE is a Research Director of the FRS-FNRS and an investigator of WELBIO. This study was supported by FMRE-Belgium, FRS-FNRS (Belgium), Interuniversity Attraction Pole (IUAP-P7/10) from Belgian Federal Scientific Affairs and Action de Recherche Concertée (FWB). The Foundation for Medical Research (FRM, Equipe FRM 2013 to PF), the Centre National de la Recherche Scientifique CNRS UMR 8246, the University Pierre et Marie Curie UM 119, Institut national de la santé et de la recherche médicale INSERM U1130. The Spanish Ministry of Economy (SAF2016-75966R-FEDER), the Generalitat de Catalunya (2014SGR34) and UE Medbioinformatic Project (grant number 634143) to OV. MN was supported by the LabEx Paris-Sciences et Lettres (PSL). The Italian Ministry of Health (RF2009-1549619) to MZ. The Fonds de la Recherche Scientifique-FNRS of the Fédération Wallonie-Bruxelles to ODB.

Author contributions

J-FDB, SM and AKE designed the experiments. J-FDB performed *ex vivo* electrophysiology, *ex vivo* voltammetry, *in situ* hybridization, behavioural paradigms and analysis on cKO, and collected all associated data. SM and AKE performed behavioural experiments on KO mice and *in situ* hybridization. BD performed stereotactic injection of AAV in PFC, LVa and JC in amygdala. AG, LVa and JC performed behavioural experiments on cKO. LC and OV performed and analysed self-administration experiments. SV and PF performed and analysed *in vivo* electrophysiology experiments. GC and MZ performed and analysed microdialysis experiments. MN and LVE performed and analysed the experiments of synaptic plasticity in the NAc. ODB provided KO and floxed *Maged1* mice. DG supervised a part of the *ex vivo* electrophysiology experiments. J-FDB, SM, OV, PF, MZ, LVE, SNS and AKE analysed the data. J-FDB and AKE wrote the

manuscript; AKE supervised all aspects of the work. J-FDB, OV, PF, MZ, LVE, SNS and AKE discussed findings, edited and contributed to the final version of the manuscript.

Conflict of interest

The authors declare that they have no conflict of interest.

References

- Volkow ND, Morales M (2015) The brain on drugs: from reward to addiction. *Cell* 162: 712–725
- Di Chiara G, Imperato A (1988) Drugs abused by humans preferentially increase synaptic dopamine concentration in the mesolimbic system of freely moving rats. *Proc Natl Acad Sci USA* 85: 5274–5278
- Lüscher C, Ungless MA (2001) The mechanistic classification of addictive drugs. *PLoS Med* 3: e437
- Lüscher C, Malenka RC (2011) Drug-evoked synaptic plasticity in addiction: from molecular changes to circuit remodeling. *Neuron* 69: 650–663
- Kourrich S, Rothwell PE, Klug JR, Thomas MJ (2007) Cocaine experience controls bidirectional synaptic plasticity in the nucleus accumbens. *J Neurosci* 27: 7321–7328
- Thomas MJ, Beurrier C, Bonci A, Malenka RC (2001) Long-term depression in the nucleus accumbens: a neural correlate of behavioral sensitization to cocaine. *Nat Neurosci* 4: 1217–1223
- Brebner K, Wong TP, Liu L, Campsall P, Gray S, Phelps L, Philips AG, Wang YT (2005) Nucleus accumbens long-term depression and the expression of behavioral sensitization. *Science* 310: 1340–1343
- Pascoli V, Turiault M, Lüscher C (2012) Reversal of cocaine-evoked synaptic potentiation resets drug-induced adaptive behaviour. *Nature* 481: 71–75
- Pascoli V, Terrier J, Espallergues J, Valjent E, O'Connor EC, Lüscher C (2014) Contrasting forms of cocaine-evoked plasticity control components of relapse. *Nature* 509: 459–464
- Dong Y, Nestler EJ (2014) The neural rejuvenation hypothesis of cocaine addiction. *Trends Pharmacol Sci* 35: 374–383
- Giros B, Jaber M, Jones SR, Wightman RM, Caron MG (1996) Hyperlocomotion and indifference to cocaine and amphetamine in mice lacking the dopamine transporter. *Nature* 379: 606–612
- van der Bruggen P, Traversari C, Chomez P, Lurquin C, De Plaen E, Van den Eynden B, Knuth A, Boon T (1991) A gene encoding an antigen recognized by cytolytic T lymphocyte on a human melanoma. *Science* 254: 1643–1674
- Bertrand MJM, Huijbers I, Chomez P, De Backer O (2004) Comparative expression analysis of *MAGED* genes during embryogenesis and brain development. *Dev Dyn* 230: 325–334
- Wang X, Tang J, Xing L, Shi G, Ruan H, Gu X, Liu Z, Wu X, Gao X, Xu Y (2010) Interaction of *MAGED1* with nuclear receptors affects circadian clock function. *EMBO J* 29: 1389–1400
- Dombret C, Nguyen T, Schakman O, Michaud JL, Hardin-Pouzet H, Bertrand MJM, De Backer O (2012) Loss of *Maged1* results in obesity, deficits of social interactions, impaired sexual behavior and severe alteration of mature oxytocin production in the hypothalamus. *Hum Mol Genet* 21: 4703–4717
- Yang JJ, Lai BB, Xu AL, Liu Y, Li XM, Zhao YN, Li WF, Ji MH, Hu G, Gao X et al (2014) *Maged1* co-interacting with CREB through a hexapeptide repeat domain regulates learning and memory in mice. *Mol Neurobiol* 51: 8–18

17. Mouri A, Sasaki A, Watanabe K, Sogawa C, Kitayama S, Mamiya T, Miyamoto Y, Yamada K, Noda Y, Nabeshima T (2012) MAGE-D1 regulates expression of depression-like behavior through serotonin transporter ubiquitylation. *J Neurosci* 32: 4562–4580
18. Grau C, Starkovich M, Azamian MS, Xia F, Cheung SW, Evans P, Henderson A, Lalani SR, Scott DA (2017) Xp11.22 deletions encompassing CENPVL1, CENPVL2, MAGED1 and GSPT2 as a cause of syndromic X-linked intellectual disability. *PLoS One* 12: e0175962
19. Renthall W, Kumar A, Xiao G, Wilkinson M, Covington HE III, Maze I, Sikder D, Robison AJ, LaPlant Q, Dietz DM et al (2009) Genome-wide analysis of chromatin regulation by cocaine reveals a role for sirtuins. *Neuron* 62: 335–348
20. Carlezon WA Jr, Duman RS, Nestler EJ (2005) The many faces of CREB. *Trends Neurosci* 28: 436–445
21. Bertrand MJM, Kenchapa RS, Andrieu D, Leclercq-Smekens M, Nguyen HNT, Carter BD, Muscatelli F, Barker PA, De Backer O (2008) NRAGE, a p75NTR adaptor protein, is required for developmental apoptosis *in vivo*. *Cell Death Differ* 15: 1921–1929
22. Everitt BJ, Robbins TW (2005) Neural systems of reinforcement for drug addiction: from actions to habits to compulsion. *Nat Neurosci* 8: 1481–1489
23. Grace AA, Bunney BS (1984a) The control of firing pattern in nigral dopamine neurons: single spike firing. *J Neurosci* 4: 2866–2876
24. Grace AA, Bunney BS (1984b) The control of firing pattern in nigral dopamine neurons: burst firing. *J Neurosci* 4: 2877–2890
25. Einhorn LC, Johansen PA, White FJ (1988) Electrophysiological effects of cocaine in the mesoaccumbens dopamine system: studies in the ventral tegmental area. *J Neurosci* 8: 100–112
26. De Mei C, Ramos M, Litaka C, Borelli E (2009) Getting specialized: presynaptic and postsynaptic dopamine D2 receptors. *Curr Opin Pharmacol* 9: 53–58
27. Koulchitsky S, De Backer B, Quertemont E, Charlier C, Seutin V (2012) Differential effects of cocaine on dopamine neuron firing in awake and anesthetized rats. *Neuropsychopharmacology* 37: 1559–1571
28. Kalivas PW (2009) The glutamate homeostasis hypothesis of addiction. *Nat Rev Neurosci* 10: 561–572
29. Kauer JA, Malenka RC (2007) Synaptic plasticity and addiction. *Nat Rev Neurosci* 8: 844–858
30. Jonas P (2000) The time course of signaling at central glutamatergic synapses. *News Physiol Sci* 15: 83–89
31. Beurrier C, Bonvento G, Kerkerian-Le Goff L, Gubellini P (2009) Role of glutamate transporters in corticostriatal synaptic transmission. *Neuroscience* 158: 1608–1615
32. Mameli M, Halbout B, Creton C, Enblom D, Rodriguez Parkitna J, Spanagel R, Lüscher C (2009) Cocaine-evoked synaptic plasticity: persistence in the VTA triggers adaptations in the NAC. *Nat Neurosci* 12: 1036–1041
33. Turiault M, Parnaudeau S, Milet A, Parlato R, Rouzeau JD, Lazar M, Tronche F (2007) Analysis of dopamine transporter gene expression pattern – generation of DAT-iCre transgenic mice. *FEBS J* 274: 3568–3577
34. Ohtsuka N, Tansky MF, Kuang H, Kourrich S, Thomas MJ, Rubenstein JLR, Ekker M, Leeman SE, Tsien JZ (2008) Functional disturbances in the striatum by region-specific ablation of NMDA receptors. *Proc Natl Acad Sci USA* 105: 12961–12966
35. Tolu S, Eddine R, Marti F, David V, Graupner M, Pons S, Baudonnat M, Husson M, Besson M, Reperant C et al (2013) Co-activation of VTA DA and GABA neurons mediates nicotine reinforcement. *Mol Psychiatry* 18: 382–393
36. Bocklisch C, Pascoli V, Wong JCY, House DRC, Yvon C, de Roo M, Tan KR, Lüscher C (2013) Cocaine disinhibits dopamine neurons by potentiation of GABA transmission in the ventral tegmental area. *Science* 341: 1521–1525
37. Kätzel D, Zelman BV, Buetfering C, Wölfel M, Miesenböck G (2011) The columnar and laminar organization of inhibitory connections to neocortical excitatory cells. *Nat Neurosci* 14: 100–107
38. Nair-Roberts RG, Chatelain-Badie SD, Benson E, White-Cooper H, Bolam JP, Ungless MA (2008) Stereological estimates of dopaminergic, GABAergic and glutamatergic neurons in the ventral tegmental area, substantia nigra and retrorubral field in the rat. *Neuroscience* 152: 1024–1031
39. Papp E, Borhegyi Z, Tomioka R, Rockland KS, Modi I, Freund TF (2012) Glutamatergic input from specific sources influences the nucleus accumbens-ventral pallidum information flow. *Brain Struct Funct* 217: 37–48
40. Everitt BJ, Robbins TW (2015) Drug addiction: updating actions to habits to compulsions ten years on. *Annu Rev Psychol* 67: 23–50
41. Wolf ME (2010) The bermuda triangle of cocaine-induced neuroadaptations. *Trends Neurosci* 33: 391–398
42. Sara Y, Bal M, Adachi M, Monteggia LM, Kavalali ET (2011) Use-dependent AMPA receptor block reveals segregation of spontaneous and evoked glutamatergic neurotransmission. *J Neurosci* 31: 5378–5382
43. Ortinski PI, Vasoler FM, Carlson GC, Pierce RC (2012) Temporally dependent changes in cocaine-induced synaptic plasticity in the nucleus accumbens shell are reversed by D1-like dopamine receptor stimulation. *Neuropsychopharmacology* 37: 1671–1682
44. Voorn P, Vanderschuren LJ, Groenewegen HJ, Robbins TW, Pennartz CM (2004) Putting a spin on the dorsal-ventral divide of the striatum. *Trends Neurosci* 27: 468–474
45. Yin HH, Mulcare SP, Hilario MRF, Clouse E, Holloway T, Davis MI, Hansson AC, Lovinger DM, Costa RM (2009) Dynamic reorganization of striatal circuits during the acquisition and consolidation of a skill. *Nat Neurosci* 12: 333–341
46. Li Y, Hu XT, Berney TG, Vartanian AJ, Stine CD, Wolf ME, White FJ (1999) Both glutamate receptor antagonists and prefrontal cortex lesions prevent induction of cocaine sensitization and associated neuroadaptations. *Synapse* 34: 169–180
47. Zavala AR, Weber SM, Rice HJ, Alleweireldt AT, Neisewander JL (2003) Role of the prelimbic subregion of the medial prefrontal cortex in acquisition, extinction, and reinstatement of cocaine-conditioned place preference. *Brain Res* 990: 157–164
48. Steinkellner T, Mus L, Eisenrauch B, Constantinescu A, Leo D, Konrad L, Rickhag M, Sorensen G, Efimova EV, Kong E et al (2014) *In vivo* amphetamine action is contingent on α CaMKII. *Neuropharmacology* 39: 2681–2693
49. Chomez P, De Backer O, Bertrand M, De Plaen E, Boon T, Lucas S (2001) An overview of the MAGE gene family with the identification of all human members of the family. *Cancer Res* 61: 5544–5551
50. Kuwajima T, Hasegawa K, Yoshikawa K (2010) Necdin promotes tangential migration of neocortical interneurons from basal forebrain. *J Neurosci* 30: 3709–3714
51. Simeone A, Acampora D, Pannese M, D'Esposito M, Stornaiuolo A, Gulisano M, Mallamaci A, Kastury K, Druck T, Huebner K et al (1994) Cloning and characterization of two members of the vertebrate Dlx gene family. *Proc Natl Acad Sci USA* 91: 2250–2254
52. Stenman J, Toresson H, Kenneth Campbell K (2003) Identification of two distinct progenitor populations in the lateral ganglionic eminence:

- implications for striatal and olfactory bulb neurogenesis. *J Neurosci* 23: 167–174
53. Katarova Z, Sekerková G, Prodan S, Mugnaini E, Szabó G (2000) Domain-restricted expression of two glutamic acid decarboxylase genes in midgestation mouse embryos. *J Comp Neurol* 424: 607–627
 54. Chu Sin Chung P, Keyworth HL, Martin-Garcia E, Charbogne P, Darcq E, Bailey A, Filliol D, Matifas A, Scherrer G, Ouagazzal AM et al (2015) A novel anxiogenic role for the delta opioid receptor expressed in GABAergic forebrain neurons. *Biol Psychiatry* 77: 404–405
 55. Almodóvar-Fabregas LJ, Segarra O, Colon N, Dones JG, Mercado M, Mejias-Aponte CA, Vazquez R, Abreu R, Vazquez E, Williams JT et al (2002) Effects of cocaine administration on VTA cell activity in response to prefrontal cortex stimulation. *Ann N Y Acad Sci* 965: 157–171
 56. Ferenczi EA, Zalocusky KA, Liston C, Grosenick L, Warden MR, Amatya D, Katovich K, Mehta H, Patenaude B, Ramakrishnan C et al (2016) Prefrontal cortical regulation of brainwide circuit dynamics and reward-related behavior. *Science* 351: aac9698
 57. Rice ME, Patel JC, Cragg SJ (2011) Dopamine release in the basal ganglia. *Neuroscience* 198: 112–137
 58. Kim IH, Rossi MA, Aryal DK, Racz B, Kim N, Uezu A, Wang F, Wetsel WC, Weinberg RJ, Yin H et al (2015) Spine pruning drives antipsychotic locomotion via circuit control of striatal dopamine. *Nat Neurosci* 18: 883–891
 59. Quiroz C, Orrú M, Rea W, Ciudad-Roberts A, Yepes G, Britt JP, Ferré S (2016) Local control of extracellular dopamine levels in the medial nucleus accumbens by a glutamatergic projection from the infralimbic cortex. *J Neurosci* 36: 851–859
 60. Chiamulera C, Epping-Jordan MP, Zocchi A, Marcon C, Cottiny C, Tacconi S, Corsi M, Orzi F, Conquet F (2001) Reinforcing and locomotor stimulant effects of cocaine are absent in mGluR5 null mutant mice. *Nat Neurosci* 4: 873–874
 61. Ghanem N, Jarinova O, Amores A, Long Q, Hatch G, Park BK, Rubenstein JL, Ekker M (2003) Regulatory roles of conserved intergenic domains in vertebrate Dlx bigene clusters. *Genome Res* 13: 533–543
 62. Soria G, Mendizabal V, Tourino C, Robledo P, Ledent C, Parmentier M, Maldonado R, Valverde O (2005) Lack of CB1 cannabinoid receptor impairs cocaine self-administration. *Neuropsychopharmacology* 30: 1670–1680
 63. Caine SB, Negus SS, Mello NK (1999) Method for training operant responding and evaluating cocaine self-administration behaviour in mutant mice. *Psychopharmacology* 147: 22–24
 64. Exley R, Maubourguet N, David V, Eddine R, Evrard A, Pons S, Marti F, Threlfell S, Cazala P, McIntosh JM et al (2011) Distinct contributions of nicotinic acetylcholine receptor subunit alpha4 and subunit alpha6 to the reinforcing effects of nicotine. *Proc Natl Acad Sci USA* 108: 7577–7582
 65. Sakae DY, Marti F, Lecca S, Vorspan F, Martin-Garcia E, Morel LJ, Henrion A, Gutierrez-Cuesta J, Besnard A, Heck N et al (2015) The absence of VGLUT3 predisposes to cocaine abuse by increasing dopamine and glutamate signalling in the nucleus accumbens. *Mol Psychiatry* 20: 1448–1459
 66. Mameli-Engvall M, Evrard A, Pons S, Maskos U, Svensson TH, Changeux JP, Faure P (2006) Hierarchical control of dopamine neuron-firing patterns by nicotinic receptors. *Neuron* 50: 911–921
 67. Benoit-Marand M, O'Donnell P (2008) D2 dopamine modulation of corticoaccumbens synaptic responses changes during adolescence. *Eur J Neurosci* 27: 1364–1372
 68. Dassesse D, Ledent C, Parmentier M, Schiffmann SN (2001) Acute and chronic caffeine administration differentially alters striatal gene expression in wild-type and adenosine A_{2A} receptor-deficient mice. *Synapse* 42: 63–76
 69. Blum D, Galas MC, Cuvelier L, Schiffmann SN (2004) Chronic intoxication with 3-nitropropionic acid in rats induces the loss of striatal dopamine terminals without affecting nigral cell viability. *Neurosci Lett* 354: 234–238
 70. Blum D, Galas MC, Gall D, Cuvelier L, Schiffmann SN (2002) Striatal and cortical neurochemical changes induced by chronic metabolic compromise in the 3-nitropropionic model of Huntington's disease. *Neurobiol Dis* 10: 410–426
 71. Durieux PF, Bearzatto B, Guiducci S, Buch T, Waisman A, Zoli M, Schiffmann SN, de Kerchove d'Exaerde A (2009) D₂R striatopallidal neurons inhibit both locomotor and drug reward processes. *Nat Neurosci* 12: 393–395